Relating Divergence in Polychaete Musculature to Different Burrowing Behaviors: A Study Using Opheliidae (Annelida)

Chris J. Law,[1,3] Kelly M. Dorgan,[1,2]* and Greg W. Rouse[1]

[1]*Scripps Institution of Oceanography, University of California San Diego, La Jolla, California 92093-0202*
[2]*Dauphin Island Sea Laboratory, Dauphin Island, Alabama 36528*
[3]*Ecology and Evolutionary Biology, University of California Santa Cruz, Santa Cruz, California 95062*

ABSTRACT Divergent morphologies among related species are often correlated with distinct behaviors and habitat uses. Considerable morphological and behavioral differences are found between two major clades within the polychaete family Opheliidae. For instance, *Thoracophelia mucronata* burrows by peristalsis, whereas *Armandia brevis* exhibits undulatory burrowing. We investigate the anatomical differences that allow for these distinct burrowing behaviors, then interpret these differences in an evolutionary context using broader phylogenetic (DNA-based) and morphological analyses of Opheliidae and taxa, such as Scalibregmatidae and Polygordiidae. Histological three-dimensional-reconstruction of *A. brevis* reveals bilateral longitudinal muscle bands as the prominent musculature of the body. Circular muscles are absent; instead oblique muscles act with unilateral contraction of longitudinal muscles to bend the body during undulation. The angle of helical fibers in the cuticle is consistent with the fibers supporting turgidity of the body rather than resisting radial expansion from longitudinal muscle contraction. Circular muscles are present in the anterior of *T. mucronata*, and they branch away from the body wall to form oblique muscles. Helical fibers in the cuticle are more axially oriented than those in undulatory burrowers, facilitating radial expansion during peristalsis. A transition in musculature accompanies the change in external morphology from the thorax to the abdomen, which has oblique muscles similar to *A. brevis*. Muscles in the muscular septum, which extends posteriorly to form the injector organ, act in synchrony with the body wall musculature during peristalsis: they contract to push fluid anteriorly and expand the head region following a direct peristaltic wave of the body wall muscles. The septum of *A. brevis* is much thinner and is presumably used for eversion of a nonmuscular pharynx. Mapping of morphological characters onto the molecular-based phylogeny shows close links between musculature and behavior, but less correlation with habitat. J. Morphol. 000:000–000, 2013. © 2013 Wiley Periodicals, Inc.

KEY WORDS: hydrostatic skeleton; muscle; polychaetes; functional morphology; locomotion

INTRODUCTION

Polychaete annelids are an abundant and morphologically diverse group of organisms that inhabit a wide range of habitats, with behaviors ranging from sessile tube-dwelling to active burrowing (Rouse and Pleijel, 2001). Even among motile polychaetes, the frequency and duration of movements vary considerably, and locomotory gaits differ among and sometimes within taxa, including parapodial crawling, undulation, and peristalsis, as well as several swimming gaits (Clark, 1964; Fauchald and Jumars, 1979). Investigation of the differences in morphological and muscular function is important for further understanding of differences in locomotory behaviors, which affect organismal distribution, performance, fitness, and habitat adaptation (Arnold, 1983; Irschick and Garland, 2001; Wainwright et al., 2008). Understanding of functional morphology underlying these burrowing behaviors has been limited by difficulty in observing infaunal organisms in situ (cf. Dorgan et al., 2006).

Body movements in many polychaetes, like in other soft-bodied animals, are achieved using a hydrostatic skeleton in which a muscular body wall surrounds a constant volume of tissues and extracellular fluids. Because fluid-filled hydrostats maintain constant volume, any change in one dimension (1D) will cause a compensatory change

Additional Supporting Information may be found in the online version of this article.

Contract grant sponsor: NSF OCE; Contract grant number: OCE-1029160; Contract grant sponsor: NSF OCE (G.W.R. and L. Levin); Contract grant number: OCE-0826254 and OCE-0939557; Contract grant sponsor: NSF Polar Programs (G.W.R., N. Wilson, and R. Burton); Contract grant number: 1043749; Contract grant sponsor: Carlsberg Foundation; Contract grant number: 2009-01-0053.

*Correspondence to: KM Dorgan; Dauphin Island Sea Laboratory, Dauphin Island, AL, 36528. E-mail: kdorgan@disl.org

Received 29 July 2013; Revised 9 October 2013;
Accepted 17 November 2013.

Published online 00 Month 2013 in
Wiley Online Library (wileyonlinelibrary.com).
DOI 10.1002/jmor.20237

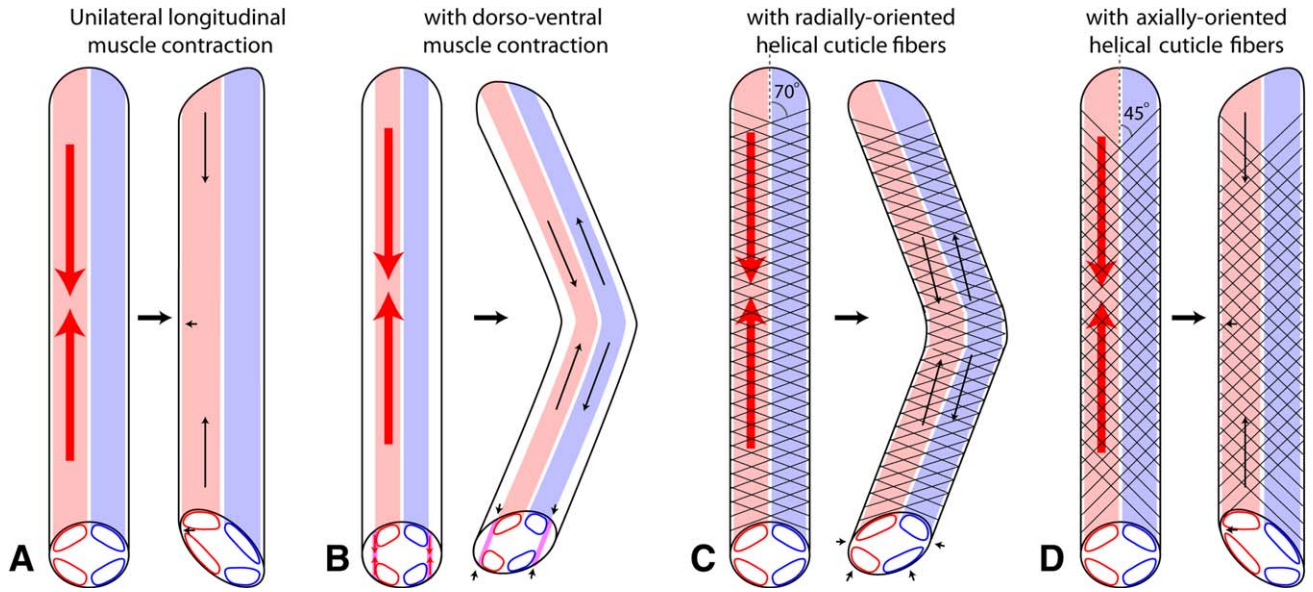

Fig. 1. (**A**) Unilateral longitudinal muscle contraction (red arrows indicate muscle contraction) with no mechanism of resisting radial expansion results in shearing of the body and longitudinal shortening (black arrows indicate body shape changes). Dorsal-ventral muscles (magenta) in *Nephtys* (**B**) and radially-oriented helical cuticle fibers (black) in *A. lumbricoides* (**C**) serve to resist radial expansion and thus resist asymmetrical longitudinal shortening and facilitate bending. Axially-oriented helical cuticle fibers (**D**) do not resist radial expansion, and thus longitudinal shortening can occur.

in at least one other dimension, and different muscle groups act antagonistically to generate body movements of elongation, shortening, bending, and torsion (Kier and Smith, 1985). In a cylindrical, worm-shaped body, muscle fibers perpendicular (circular, transverse, oblique) and parallel (longitudinal) to the long axis control the diameter and length, respectively (Kier, 2012). Locomotion by peristalsis, well-documented in earthworms and other vermiform animals, involves either alternating or simultaneous waves of contractions of longitudinal and circular muscles in the body wall, in which contraction of longitudinal muscles expands the body radially and contraction of circular muscles elongates and extends the body anteriorly (Gray and Lissmann, 1938; Trueman, 1966; Seymour, 1976; Elder, 1980).

A growing number of polychaete taxa, however, have been found to have body walls inconsistent with the traditionally described (e.g., Lanzavecchia et al., 1988; Gardiner, 1992) outer layer of circular muscles and inner layer of longitudinal muscles. Rather, many polychaetes lack circular muscle fibers along part, or even all of the body (Tzetlin and Filippova, 2005; Purschke and Müller, 2006). Some of these taxa also exhibit nonperistaltic locomotory behaviors such as undulation (Clark and Clark, 1960; Clark and Hermans, 1976; Dorgan et al., 2013). Bending movements do not require circular musculature and, instead, are achieved by unilateral contraction of longitudinal muscles. Unilateral longitudinal contraction alone would result in shearing of the body; some mechanism of resisting radial expansion is necessary to prevent an asymmetrical increase in body thickness and resultant longitudinal shortening (Kier, 2012). In the polychaete *Nephtys* (Nephtyidae), dorsal-ventral muscles act to prevent radial expansion and enable bending (Clark and Clark, 1960), whereas in the nematode *Ascaris lumbricoides*, a helical array of inextensible fibers in the cuticle serves a similar function (Harris and Crofton, 1957; Fig. 1).

Considerable behavioral differences are found between the two major clades within the polychaete family Opheliidae, where species in Ophelininae move by undulation and those in Opheliinae use peristaltic locomotion (Rouse and Pleijel, 2001). These behavioral differences are accompanied by clearly distinctive morphologies (Fig. 2) and habitats. The two clades are represented in this study by *Armandia brevis* and *Thoracophelia mucronata*, respectively. *A. brevis* both burrows and swims using undulatory movements (Clark and Hermans, 1976; Dorgan et al., 2013) and has a smooth, rigid body with ventral and lateral grooves extending along the entire length. It is found in surficial ($<$ 3 cm) heterogeneous sediments (Woodin, 1974; Hermans, 1978). Most macrofaunal burrowers in muddy sediments use eversible mouth parts or muscular anterior regions to apply dorsoventral forces to burrow walls and extend the burrow by fracture (Dorgan et al., 2005, 2006). *A. brevis*, however, lacks the morphological features consistent with this mechanism and, instead, uses body undulations (Fig. 2A) to plastically rearrange sediments (Dorgan et al.,

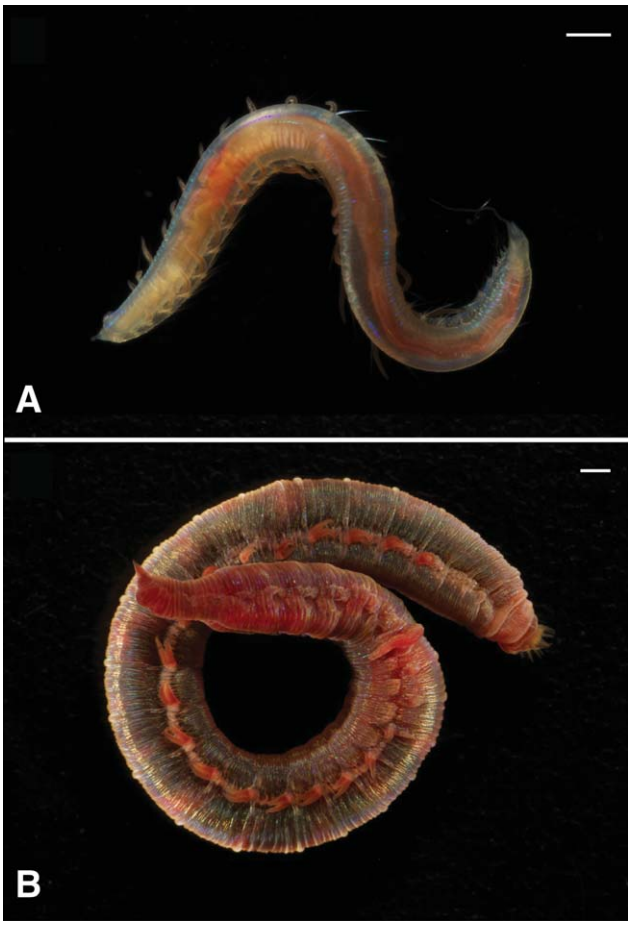

Fig. 2. Live adult specimens of (**A**) *Armandia brevis* (Ophelininae), found in surficial heterogenous sediments and exhibits undulating locomotion, and (**B**) *Thoracophelia mucronata* (Opheliinae), found in high intertidal sandy beaches and exhibits peristaltic locomotion. Each species represents one of the two clades within Opheliidae. Scale bar = 1 mm.

2013). This mechanism is likely limited to uncompacted, surface sediments, consistent with habitat descriptions for *A. brevis*. *T. mucronata* (Fig. 2B) is found in the high intertidal on sandy beaches, in distinct zones of high abundance (McConnaughey and Fox, 1949). It burrows by direct peristalsis, with the wave of contraction traveling anteriorly, and has a body divided into distinct regions: 1) an anterior cephalic region consisting of the prostomium and first two chaetigers; 2) a swollen thoracic region; and 3) a tapering posterior region with ventral and lateral grooves. A lateral notopodial ridge separates the thoracic and posterior regions at the 10th chaetiger (Blake, 2000; Santos et al., 2004; Law et al., 2013).

The substantial differences between these opheliid species in external morphology, behavior, and habitat suggest a divergence in underlying musculature as well. *A. brevis* has longitudinal and oblique muscles, but lacks circular muscles, and has an open body cavity with two to –three anterior septa (Clark and Hermans, 1976; Tzetlin and Zhadan, 2009). The posterior region of *T. mucronata* has similar general musculature to *A. brevis* (Hartmann-Schröder, 1958; Clark and Hermans, 1976), whereas circular muscles have been described in the anterior region (Hartmann-Schröder, 1958). *T. mucronata* also has an open body cavity, but with anterior septa that extend over the esophagus to form the "injector organ" (McConnaughey and Fox, 1949). Here, we directly compare musculature of *A. brevis* and *T. mucronata* and relate muscle structure to locomotory function for each species. We focus specifically on 1) the change in musculature at the transition region from the thorax of *T. mucronata* to the abdomen, over which circular muscles disappear, 2) the anterior septa, and 3) the oblique muscles in the posterior of *T. mucronata* and the entire body of *A. brevis*.

Inextensible helical fibers in the cuticle of hydrostats resist changes in body shape, with more circumferentially oriented fibers resisting radial expansion caused by longitudinal muscle contraction (facilitating undulatory movement) and fibers oriented at small angles from the longitudinal body axis resisting elongation (facilitating peristalsis), with an angle of 54° 44′ intermediate between the two (Kier, 2012; Wainwright et al., 1976; Fig. 1C,D). Circumferentially oriented cuticle fibers (∼75° from the body axis) in the nematode, *A. lumbricoides*, prevent radial expansion so that unilateral longitudinal muscle contraction results in bending (Harris and Crofton, 1957; Fig. 1C). Clark and Hermans (1976) found that cuticle fibers in the undulatory-moving opheliid, *Ophelina* sp., have angles ∼55° from the longitudinal body axis, and they suggested that bending is enabled by oblique muscles rather than the cuticle fibers. We compare cuticle fiber angles between the undulatory-burrowing and peristaltic-burrowing opheliids, hypothesizing that cuticle fiber angles will be smaller than 54° 44′ in the anterior of *T. mucronata* to enable radial expansion during peristalsis.

We also construct an opheliid phylogeny based on DNA sequences to generalize the morphologies and behaviors of *A. brevis* and *T. mucronata* described in this study across Opheliidae. The morphologically similar Polygordiidae and the closely related Scalibregmatidae were incorporated for broader comparison. Polygordiids have been suggested to be close to or part of Opheliidae based on similar morphological characteristics such as cuticle, muscular organization, and undulatory locomotion (McIntosh, 1875; Clark and Hermans, 1976; Giard, 1880) and *Travisia* was recently moved from Opheliidae to Scalibregmatidae (Paul et al., 2010), reflecting similar morphological characters such as body shape and epidermal rugosity that have linked *Travisia* with

Scalibregmatidae for over a century (Ashworth, 1901). All three families share the presence of a ventral groove and mostly nonseptate bodies. Using the phylogeny, we generate here, we map morphological characters to examine broader relationships among external morphologies, musculature, and burrowing behavior and habitat. Several additional taxa, notably Terebellidae (Nogueira et al. 2010) and *Pisionidens* (Sigalionidae) (Aiyar and Alikunhi, 1940; Tzetlin, 1987; Norlinder et al., 2012), exhibit ventral or dorsal grooves, suggesting that broader analyses of these characteristics across annelids may be useful, but as this study focuses on morphological divergence, we limit our analysis to taxa closely related to opheliids (cf. Struck et al. 2006, 2011). Moreover, most Terebellidae are sessile tube dwellers rather than active burrowers (Fauchald and Jumars, 1979), and the ventral groove in this group may serve another purpose.

In this study, we use morphological data from histology, 3D-reconstructions of thin sections, live microscopy, and cuticle fiber angle measurements, as well as DNA-based phylogenetic analyses to 1) describe the musculature and morphological features used for locomotion within Opheliidae, using *A. brevis* and *T. mucronata* as representatives of the two major opheliid clades; 2) relate these muscular and morphological features to disparate forms of burrowing and behavior; and 3) investigate broader morphological comparisons among Opheliidae, Scalibregmatidae, and Polygordiidae.

MATERIALS AND METHODS

Histology

A. brevis (Moore, 1906) and *T. mucronata* (Treadwell, 1914) were collected from Mission Bay, San Diego, California on June 9, 2011 and La Jolla Shores Beach, California on May 4, 2012, respectively. Specimens (10) of each species were relaxed in 7.5% $MgCl_2$ and fixed in 4% glutaraldehyde buffered with 0.2 mol l^{-1} sodium cacodylate with 0.3 mol l^{-1} sucrose for 24 h. The specimens were then rinsed in buffer and dehydrated in a graded series of ethanol rinses and embedded in low viscosity Spurr's resin, following manufacturer's instructions (Spurr, 1969). Semithin serial cross-sections of specimens were prepared using a Histo diamond knife (DiATOME) on a PowerTome Ultramicrotome (Boeckeler Instruments) and stained with Toluidine blue. A total of four specimens, two each of *A. brevis* and *T. mucronata*, were sectioned at a thickness of 1.5 μm for histological 3D-reconstruction, and two *A. brevis* specimens were sectioned sagittally at a thickness of 3 μm to visualize anterior septa. Serial sections were photographed using either a Canon Powershot G9 camera attached to a Leica DMR microscope or a Canon T1i camera attached to an Olympus CX41 microscope. Selected sections were viewed with a Zeiss AxioObserver Z1 microscope with DIC filters and AxioVision software to photograph finer details of the connectivity and transitions between circular and oblique musculature in both worms.

3D-Reconstruction and Visualization

AMIRA 5.4 (Visage Imaging) running on MAC OS v.10.6.8 was used for all 3D-reconstructions, following procedures modified from Ruthensteiner (2008). Every other section, equaling 3-μm increments, of the *A. brevis* specimen was photographed, and every fourth section, equaling 6-μm increments, of the *T. mucronata* specimen was photographed. Before importing into AMIRA for 3D-reconstruction, section images were reduced in size, converted to grayscale, contrast enhanced, and color inverted using Adobe Photoshop CS5; color inversion is necessary for volume rendering in AMIRA. A 3D-reconstruction of the region of four anterior chaetigers of *A. brevis* (excluding the head region) targeted the following morphologies and musculature: dorsal longitudinal muscles, ventral longitudinal muscles, oblique muscles, and ventral nerve cord. For *T. mucronata*, 3D-reconstructions of Chaetigers 2–9 focused on the body cavity and septum/injector organ and of Chaetigers 9–14 on the body cavity and lateral ridge. The least-squares alignment mode was initially used to align the sections, followed by manual adjustments when necessary. The Segmentation Editor was used to create the 3D-images of structures. Labeling of structures was done by hand on every third slice followed by interpolation to connect intermediate slices. Resampling and separation of the structures, labeled in Amira as "materials", were performed prior to surface rendering to decrease file output size. Surface rendering was performed with the SurfaceGen module under unconstrained smoothing at default settings followed by the SmoothSurface module to improve surface quality with iterations of >80. The Volren module was used to visualize external features of both specimens. Dimensions were adjusted so 1 model unit equaled 1 μm.

The 3D-model was embedded into a PDF file with the 3D Reviewer and 3D-Toolkit extensions found in Adobe Acrobat 9 Pro Extended running on Windows XP. Each 3D-object was saved as a separate Wavefront OBJ-file in AMIRA and recombined as one model in the 3D, Reviewer by importing one OBJ-file at a time. Objects were color edited and transferred to the 3D toolkit as a PDF for further editing of orientation, rendering style, background color, and lighting.

Fiber Angle Measurements

Cuticle fiber angles were measured in anterior, mid-body, and posterior regions, on dorsal and ventral sides of *T. mucronata* and *Ophelina acuminata* (Örsted, 1843), a species morphologically and behaviorally similar to *A. brevis* but larger and much easier to dissect. *O. acuminata* were collected from fine-grained subtidal sediments in Friday Harbor, Washington, and *T. mucronata* from La Jolla Shores Beach, California. Four O. acuminata and three T. mucronata were anesthetized in 7.5% $MgCl_2$, fixed in a phosphate-buffered mixture of 3% glutaraldehyde and 3% paraformaldehyde, then rinsed in distilled water overnight, frozen at $-20°C$ overnight to facilitate separation of cuticle from muscle tissue (Murray et al., 1981), and thawed in distilled water. In addition, five unpreserved *T. mucronata* were anesthetized in the freezer, frozen overnight, and thawed in distilled water. The cuticle was removed from different regions of the body, mounted on slides with a drop of distilled water, and visualized with polarized microscopy (Fig. 3). Angle of fibers from the longitudinal axis of the body was measured as half of the total angle between crossed fibers. Orientation of the cuticle was obvious from circumferential grooves (visible as lines) separating segments.

Peristaltic Movements

To observe the movements of the septum and injector organ corresponding with the peristaltic wave, live *T. mucronata* were placed in tunnels in a thin layer of seawater gelatin between a microscope slide and cover slip. Tunnels were created by allowing the gelatin to set around straight pieces of fishing line, which were then pulled out of the set gelatin. Small worms with diameter close to that of the fishing line were positioned with the anterior at the entry of the tunnel and encouraged to move. Videos were recorded using a Canon T3i attached to a Leica DMR microscope with polarizing filters (see Supporting Information, S-Movie). Crossed polarizers were used to view

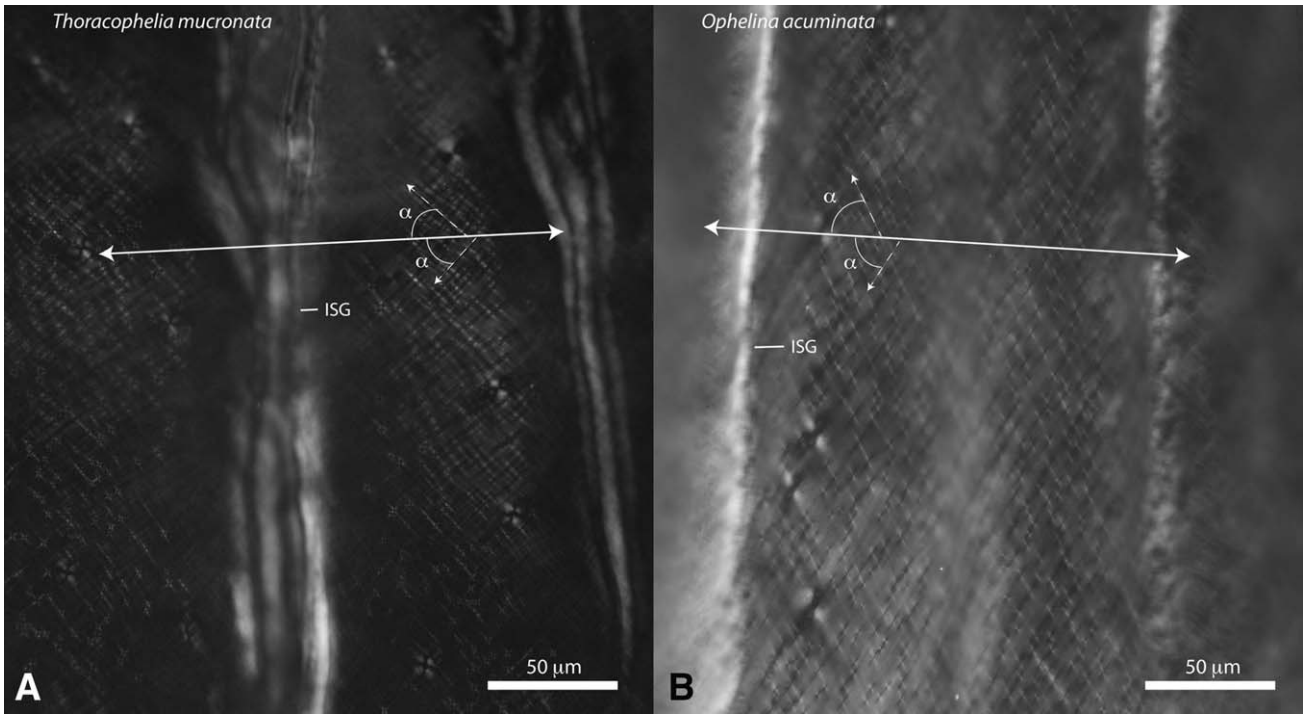

Fig. 3. Polarized images of cuticle from the anterior region of (**A**) *Thoracophelia mucronata* and (**B**) *Ophelina acuminata* with intersegmental groove (ISG) indicated. The body axis, indicated with the double-arrowed white line, is perpendicular to the intersegmental grooves. Crossed helical fibers of the cuticle are visible between intersegmental grooves, with one fiber traced with a dotted line on either side of the body axis line and fiber angle indicated as α. Scale bar = 50 μm.

muscle fibers, which are birefringent. Movements of internal structures and musculature as the worm moved through the tunnel were described, with emphasis on the synchrony between the body wall peristaltic wave and the musculature of the septum and injector organ.

DNA Amplification and Sequencing

Forty one specimens of 33 species were used for phylogenetic analyses: 25 opheliids, four polygordiids, and 10 scalibregmatids. The two outgroup taxa, a capitellid *Notomastus* sp. and an arenicolid *A. marina* were chosen based on Struck et al.'s (2011) annelid phylogeny (Table 1) with *Notomastus* sp. being used as the root terminal. Newly collected specimens [from Beaufort, NC (*Ophelina* sp1.); Costa Rica (*Ophelina* sp3.); Friday Harbor, WA (*Notomastus* sp., *O. acuminata*, *Polygordius* sp., and *Scalibregma inflatum*); Greenland (*O. acuminata, O. cylindricaudata*, and *O. limacina*); La Jolla, CA (*A. brevis*, *Polyophthalmus* sp., and *T. mucronata*); Lizard Island, Australia (*Armandia* sp1.); and off the Oregon coast (*Ophelina* sp2.)] were relaxed in 7.5% $MgCl_2$ and fixed in 95% ethyl alcohol. Sequences for the remaining 26 species were accessed through GenBank (Table 1).

A Qiagen DNeasy tissue kit was used to extract genomic DNA from specimens according to the manufacturer's instructions. Approximately 500 base pairs of the mitochondrial small subunit ribosomal DNA (16S) were amplified using the primers 16SarL and 16SbrL (Palumbi, 1996) with temperature profiles of 95°C for 3 min, followed by 40 cycles of 95°C for 40 s, 48°C for 40 s, 68°C for 50 s, and final extension at 68°C for 5 min (see Supporting Information, Table S1).

Three nuclear loci were also sequenced. The small subunit ribosomal DNA (18S) was amplified using three primer sets: 1) 1F and 5R; 2) 3F and bi; and 3) a2.0 and 9R (Giribet et al., 1996, 1999). Temperature profiles for the 1F/5R and a2.0/9R primer sets were 95°C for 3 min, followed by 40 cycles of 95°C for 30 s, 52°C for 30 s, 72°C for 90 s, and final extension at 72°C for 8 min. The temperature profile for the 3F/bi primer set was 95°C for 3 min, followed by 40 cycles of 95°C for 30 s, 49°C for 30 s, 72°C for 90 s, and final extension at 72°C for 8 min. Approximately 930 base pairs of the large subunit ribosomal DNA (28S) were amplified using the primers Po28F1 and Po28R4 (Struck et al., 2006), and ~360 base pairs of the nuclear protein coding gene Histone H3 were amplified using the primers H3aF and H3aR (Colgan et al., 1998). Both genes were amplified using the same temperature profiles of 94°C for 2 min, followed by 35 cycles of 94°C for 45 s, 48°C for 60 s, 72°C for 90 s, and final extension at 72°C for 10 min.

Amplification reactions (25 μl) were conducted containing 2 μl of DNA template, 1 μl of forward and reverse primers, 12.5 μl GoTaq Green Master Mix (Promega), and 8.5 μl H_2O. ExoSAP-IT (Affymetrix) was used to purify PCR products. Sequencing was done by either Retrogen (San Diego, CA) or Eurofins MWG Operon (Louisville, KY). Sequences were edited using Geneious 5.5.6 (www.geneious.com) and aligned with MAFFT 3.8 (Katoh and Kuma, 2002) under default settings with no manual alterations. The combined molecular dataset consisted of 3,955 total characters, 1,075 of which were parsimony informative and 436 were uninformative.

Phylogenetic Analysis

Parsimony analyses on the combined genes (16S, 18S, 28S, and H3) were conducted in PAUP* 4.0b10 (Swofford, 2002) using a heuristic search with random stepwise addition of the terminals for 1,000 replicates, with tree bisection and reconnection. The character matrix was equally weighted, and gaps were treated as missing data. Clade support was assessed using jackknifing with 37% deletion of sites over 1,000 replicates with 10 random additions per iteration. Maximum likelihood analyses were performed in RAxML 7.2.8 (Stamatkis, 2006) as a four-gene partitioned dataset and under the General Time Reversible + Gamma (GTR + G) model. Bootstrap (thorough

TABLE 1. GenBank and voucher accession numbers

Taxon	Specimen origin	Voucher	16S	18S	28S	H3
Arenicolidae						
Arenicola marina, Linnaeus (1748)	Arcachon, France[a]	–	AY532328	AF508116	AY612629	DQ779718
Capitellidae						
Notomastus sp., Hendel (1935)	Friday Harbor, WA, USA	A3421	**KF511858**	**KF511859**	**KF511860**	**KF511880**
Opheliidae						
Armandia bilobata, Hartmann-Schroder (1986)	South Australia[b]	–	DQ779604	DQ779641	DQ779676	DQ779719
Armandia brevis, Moore (1906)	La Jolla, CA, USA	A3411	**KF511804**	**KF511818**	**KF511838**	**KF511861**
Armandia brevis, Moore (1906)	Friday Harbor, WA, USA[c]	–	HM746708	EU418854	HM746736	HM746752
Armandia maculata, Webster (1884)	Twin Cayes, Belize[c]	–	–	–	HM746737	HM746753
Armandia sp.	Lizard Island, Great Barrier Reef	A3412	**KF511806**	**KF511820**	**KF511843**	**KF511866**
Ophelia bicornis, Savigny (1818)	Arcachon, France[c]	–	–	AF508122[d]	HM746745	HM746762
Ophelia limacina, Rathke (1843)	Greenland	A3403	**KF511817**	**KF511829**	**KF511850**	**KF511868**
Ophelia neglecta, Schneider (1892)	Concarneau, France[c]	–	HM746718	AF448156[d]	HM746747	HM746764
Ophelia rathkei, Mcintosh (1908)	North Sea island of Sylt, Germany[e]	–	–	AF448157[e]	AY366513	–
Ophelina acuminata (CA), Orsted (1843)	Southern CA, USA	A3413	**KF511810**	**KF511825**	**KF511839**	**KF511869**
Ophelina acuminata (Eur), Orsted (1843)	Helgoland, Germany[c]	–	HM746716	HM746735	HM746744	HM746761
Ophelina acuminata (Eu), Orsted (1843)	Europe	A3414	**KF511811**	**KF511826**	**KF511840**	–
Ophelina acuminata (FH), Orsted (1843)	Friday Harbor, WA, USA	A3404	**KF511812**	**KF511827**	**KF511842**	**KF511870**
Ophelina acuminata (GR), Orsted (1843)	Greenland	A3415	**KF511813**	**KF511828**	**KF511841**	**KF511871**
Ophelina cylindricaudata (NE), Hansen (1878)	New England, USA[c]	–	HM746717	HM746730	HM746746	HM746763
Ophelina cylindricaudata (GR), Hansen (1878)	Greenland	A3416	–	**KF511824**	**KF511848**	**KF511865**
Ophelina sp1.	Beaufort, NC, USA	A3417	**KF511814**	**KF511834**	**KF511849**	**KF511876**
Ophelina sp2.	Oregon, USA	–	**KF511807**	**KF511822**	**KF511845**	**KF511862**
Ophelina sp2.	Oregon, USA	A3418	**KF511808**	**KF511821**	**KF511846**	**KF511863**
Ophelina sp3.	Costa Rica	–	**KF511809**	**KF511823**	**KF511847**	**KF511864**
Polyophthalmus pictus, Dujardin (1839)	Lemon Tree Passage, Australia[f]	–	–	AB106267	AF185171	AF185259
Polyophthalmus sp.	La Jolla, CA, USA	A3419	**KF511805**	**KF511819**	**KF511844**	**KF511867**
Thoracophelia bibranchia, Hutchings and Murray (1984)	Merewether Beach, Australia[f]	–	–	–	AB106266	–
Thoracophelia ezoensiss, Okuda (1963)	Esashi, Japan[c]	_	_	HM746725	HM746738	HM746755
Thoracophelia mucronata (LJ), Treadwell (1914)	La Jolla, CA, USA	A3409	–	**KF511831**	**KF511852**	**KF511873**
Polygordiidae						
Polygordius appendiculatus, Fraipont (1887)	North Sea Island Helgoland, Germany[g]	–	–	AY525629	EU418872	–
Polygordius jouinae, Ramey et al. (2006)	Beach Haven Ridge, New Jersey, USA[h]	–	–	DQ153064	–	–
Polygordius lacteus, Schneider (1868)	Brittany, France[b]	–	DQ779633	DQ779669	DQ779707	DQ779757
Polygordius sp	Friday Harbor, WA, USA		**KF511815**	**KF511835**	**KF511855**	**KF511879**
Scalibregmatidae						
Hyboscolex pacificus, Moore (1909)	Santa Barbara, CA, USA[c]	–	HM746712	AB106268	HM746740	HM746757
Lipobranchius jeffreysii, McIntosh (1869)	Unknown[d]	–	–	AF508120	–	–
Neolipobranchius sp.,	Gulf of Maine, USA[a]	–	–	AY612616	AY612626	–

Table 1. (continued).

Taxon	Specimen origin	Voucher	16S	18S	28S	H3
Polyphysia crassa, Orsted (1843)	Tjaerno, Sweden[c]	–	HM746719	HM746731	HM746748	HM746765
Scalibregma inflatum (Eu), Rathke (1843)	Helgoland, Germany[c]	–	AY532331	AF448163	AY612624	DQ779764
Scalibregma inflatum (FH), Rathke (1843)	Friday Harbor, WA, USA	A3420	**KF511816**	**KF511837**	**KF511857**	**KF511877**
Sclerobregma branchiata, Hartman (1965)	Gulf of Maine, USA[d]	–	–	AY612615	AY612623	–
Travisia brevis, Moore (1923)	Friday Harbor, WA, USA[e]	–	HM746721	AY966901	HM746749	HM746767
Travisia kerguelensis, McIntosh (1885)	Antarctica		–	**KF511836**	**KF511856**	**KF511878**
Travisia pupa, Moore (1906)	Bamfield, Canada[c]	–	HM746722	HM746733	HM746750	HM746768

GenBank numbers in bold indicate new sequences.
[a]Bleidorn (2005).
[b]Rousset et al. (2007).
[c]Paul et al. (2010).
[d]Bleidorn et al. (2003).
[e]Jordens et al. (2004).
[f]Hall et al. (2004).
[g]Stuck et al. (2008).
[h]Ramey et al. (2006).
[i]Persson and Pleijel (2005).

option) values were estimated using 100 pseudoreplicates under the same model.

Characters for Transformations

A behavioral and morphological character matrix was compiled to relate burrowing mode with distinctive morphology and musculature across the DNA-generated phylogeny (Tables 2 and 3). We constructed nine characters based on key morphological and behavioral features that underlie the different locomotory behaviors exhibited by *A. brevis* and *T. mucronata*. The nine characters, with character states given in brackets, are shown below as a brief outline for each feature. Characters were only assigned states based on direct evidence found in the literature or on observations from this study with exception of Characters 1–3 (burrowing), where unknown burrowing states were generalized over genera. Characters with unknown states are indicated with a "?". Characters that were inapplicable for a given terminal are indicated by "-" (treated the same as "?"). Justifications and references for the scoring of each terminal are provided in Supporting Information, Appendix A. The burrowing behavioral and morphological characters were traced onto the tree generated by the maximum likelihood analysis using most parsimonious transformations implemented in Mesquite 2.75 (Maddison and Maddison, 2011).

Burrowing. *Burrowing mode [(0) peristaltic (1) undulatory].* Many polychaetes with diverse morphologies burrow by peristalsis, in which a wave of muscular contraction moving anteriorly or posteriorly results in movement of the body (Trueman, 1978). Some polychaetes, such as *A. brevis* and *O. acuminata*, use undulatory body movements rather than peristalsis to move (Clark and Hermans, 1976; Dorgan et al., 2013).

Type of peristalsis [(0) direct (1) retrograde]. Peristaltic locomotion can be categorized into two general types: retrograde peristalsis, in which the peristaltic wave travels in the opposite direction of locomotion, and direct peristalsis, in which the peristaltic wave travels in the same direction as locomotion (Elder, 1980). For direct peristalsis to result in forward movement, simultaneous contractions of longitudinal and circular musculature must move fluid through the body cavity. Direct peristalsis is thus limited to animals with open body cavities such as *T. mucronata* (e.g., Wells, 1961; Elder, 1973). Retrograde peristalsis, on the other hand, can occur both in segmented animals divided by septa and those with open body cavities, (e.g., Seymour, 1976).

Proboscis use during burrowing [(0) absent (1) present]. For worms burrowing in muds, eversion of a pharynx or proboscis applies a dorsoventral force on the burrow walls that is amplified at the crack tip, resulting in burrow extension by fracture (Dorgan et al., 2005; Murphy and Dorgan, 2011). Arenicolids evert their axial nonmuscular proboscises (Tzetlin and Purschke, 2005) for initial penetration into the sediment and further deepening of their burrows (Trueman, 1966). Both *A. brevis* and *T. mucronata* have nonmuscular pharynges that are, however, not used during burrowing.

Musculature. *Circular muscles [(0) absent (1) present but restricted to anterior (2) present along entire body].* Polychaete musculature has traditionally been described as consisting of an outer layer of circular muscles between the epidermis and longitudinal muscles (Lanzavecchia et al., 1988; Gardiner, 1992). Opheliids, however, lack circular muscle in part or all of the body (Hartmann-Schroder, 1958; Clark and Hermans, 1976), Polygordiids also have

TABLE 2. Summary of morphological characters

Burrowing
1. Burrowing mode: (0) peristaltic; (1) undulatory.
2. Type of peristalsis: (0) direct; (1) retrograde.
3. Proboscis use during burrowing: (0) absent; (1) present.

Musculature
4. Circular muscles: (0) absent; (1) present, but restricted to anterior; (2) present, along entire body.
5. Oblique muscles: (0) absent; (1) present.

Septa
6. Septa: (0) along the entire body; (1) 3 −5 anterior septa; (2) 1—2 anterior septa.
7. Modified anterior septa: (0) absent; (1) present.

Habitat distribution
8. Sand/mud habitat distribution: (0) sand; (1) mud.

External morphologies
9. Ventral groove (0) absent; (1) present, but restricted to posterior; (2) present, along the entire length of body.

TABLE 3. Character matrix

	Characters								
Terminal	1	2	3	4	5	6	7	8	9
Arenicolidae									
Arenicola marina	0	0	1	2	0	1	1	0	0
Capitellidae									
Notomastus sp.	0	1	1	2	0	0	1	1	0
Opheliidae									
Armandia bilobata	1	—	0	?	?	?	?	0	2
Armandia brevis (SD)	1	—	0	0	1	2	0	1	2
Armandia brevis (FH)	1	—	0	0	1	2	0	1	2
Armandia maculata	1	—	0	?	?	?	?	1	2
Armandia sp.	1	—	0	?	?	?	?	?	2
Ophelia bicornis	0	?	?	1	1	2	1	0	1
Ophelia limacina	0	?	?	1	1	?	?	0	1
Ophelia neglecta	0	?	?	1	1	2	1	0	1
Ophelia rathkei	0	?	?	1	1	?	?	0	1
Ophelina acuminata (CA)	1	—	0	0	1	?	?	1	2
Ophelina acuminata (EU)	1	—	0	0	1	?	?	1	2
Ophelina acuminata (FH)	1	—	0	0	1	?	?	1	2
Ophelina acuminata (GER)	1	—	0	0	1	?	?	1	2
Ophelina acuminata (GR)	1	—	0	?	?	?	?	1	2
Ophelina cylindricaudata (GR)	1	—	0	?	?	?	?	1	2
Ophelina cylindricaudata (NE)	1	—	0	0	1	?	?	1	2
Ophelina sp1.	1	—	0	?	?	?	?	1	2
Ophelina sp2.	1	—	0	?	?	?	?	1	2
Ophelina sp2.	1	—	0	?	?	?	?	1	2
Ophelina sp3.	1	—	0	?	?	?	?	1	2
Polyophthalmus pictus	1	—	0	0	1	?	?	0	2
Polyophthalmus sp.	1	—	0	0	1	?	?	0	2
Thoracophelia bibranchia	0	0	0	?	1	?	?	0	1
Thoracophelia ezoensiss	0	0	0	?	1	?	?	0	1
Thoracophelia mucronata	0	0	0	1	1	2	1	0	1
Polygordiidae									
Polygordius appendiculatus	1	—	0	2	1	0	0	0	2
Polygordius jouinae	1	—	0	?	?	?	?	0	2
Polygordius lacteus	1	—	0	0	1	0	0	0	2
Polygordius sp	1	—	0	?	1	0	0	0	2
Scalibregmatidae									
Hyboscolex pacificus	0	0	?	?	?	?	?	1	0
Lipobranchius jeffreysii	0	0	?	?	?	?	?	1	?
Neolipobranchius sp.	0	0	?	?	?	?	?	1	?
Polyphysia crassa	0	0	0	2	1	1	?	1	0
Scalibregma inflatum (EU)	0	0	?	2	1	1	0	1	1
Scalibregma inflatum (FH)	0	0	?	2	1	1	0	1	1
Sclerobregma branchiata	0	0	?	?	?	?	?	?	0
Travisia brevis	0	?	?	2	1	?	?	1	0
Travisia kerguelensis	0	?	?	?	?	?	?	1	0
Travisia pupa	0	?	?	2	1	1	0	1	0

traditionally been described with absent circular muscles (Fraipont, 1887); however, a recent study shows "minute" circular muscles occur in *Polygoridus appendiculatus* (Lehmacher et al., in press).

Oblique muscles [(0) absent (1) present]. Oblique muscles are present in some polychaete groups, running from the midventral line on either side of the ventral nerve cord to the midlateral region (Rouse and Pleijel, 2001).

Septa. *Septa [(0) along the entire body (1) 3–5 anterior septa (2) 1–2 anterior septa].* Septa are uniform throughout the body in most polychaetes (Fauchald and Rouse, 1997). However, some polychaetes are unusual in having only anterior septa and reduced or absent posterior septa, which seals off the head from the remaining undivided body cavity (Ashworth, 1904; Dales, 1962; Hunter et al., 1983; this study).

Modified anterior septa [(0) absent (1) present]. We define a modified septum as a muscularized anterior septum that is associated with anterior eversible structures. In *Ophelia* and *Thoracophelia*, these anterior septa extend toward the posterior to form the injector organ (Brown, 1938; McConnaughey and Fox, 1949; Harris, 1994; this study). Similarly, a muscularized septum extends posteriorly in arenicolids and capitellids to form the gular membrane (Eisig, 1887; Wells, 1954; Dales, 1962).

Habitat distribution. *Sand/mud habitat distribution [(0) sand (1) mud].* Mechanical responses of granular sands and elastic cohesive muds to forces applied by burrowers differ (Dorgan et al., 2006). Habitat is characterized based on personal observations or literature descriptions.

External morphologies. *Ventral groove [(0) absent (1) present but restricted to posterior (2) present along entire body].* Opheliids are characterized by the presence of a ventral groove along the entire length of the body or restricted to just the posterior (Blake, 2000). Polygordiids also exhibit a ventral groove along the entire length of the body (Rota and Carchini, 1999).

RESULTS

Morphology and Musculature

***A. brevis* (and *O. acuminata*).** The body is not divided into distinct body regions and shows deep ventral and lateral grooves along the entire length (Figs. 2A,4A). Internally, large dorsal and ventral longitudinal muscle bands lie directly beneath the epidermis (Fig. 4B,C). The ventral longitudinal muscles form two well-developed ventral bundles that shape the ridges of the ventral groove and are separated by the ventral nerve cord (Fig. 4B,G). The dorsal longitudinal muscle bands become thinner middorsally but do not separate completely. No circular muscle fibers are found between the epidermis and longitudinal muscles, but four bands of oblique muscle occur per segment (Fig. 4D,E). Oblique muscle bands extend from just dorsal of the ventral nerve cord and attach to the lateral epidermis between the dorsal and ventral longitudinal muscles (Fig. 4F–H).

The only septa present occur in the anterior region, where two septa occur just posterior to the pharynx (Fig. 4I). The remaining body cavity is undivided by septa, allowing coelomic fluids to flow freely during body movements.

The angle between the helical fibers of the cuticle and the longitudinal axis in *O. acuminata* is not significantly different from 54° 44′ in the anterior (t-test, $P > 0.05$) and only slightly lower in the posterior ($52.4 \pm 0.2°$ (mean ± s.d.); t-test, $P = 0.002$; Fig. 5).

***T. mucronata*.** The body is divided into three distinct regions, i.e., the head (prostomium, peristomium, and chaetigers 1–2), thorax (Chaetigers 3–10), and abdomen (Chaetigers 11–38); a pair of lateral ridges occur at Chaetiger 10 and a ventral groove is present only along the abdomen (Figs. 2B, 6A, and 7). Dorsal and ventral longitudinal muscles run along the entire length of the body. The ventral nerve cord separates the ventral longitudinal

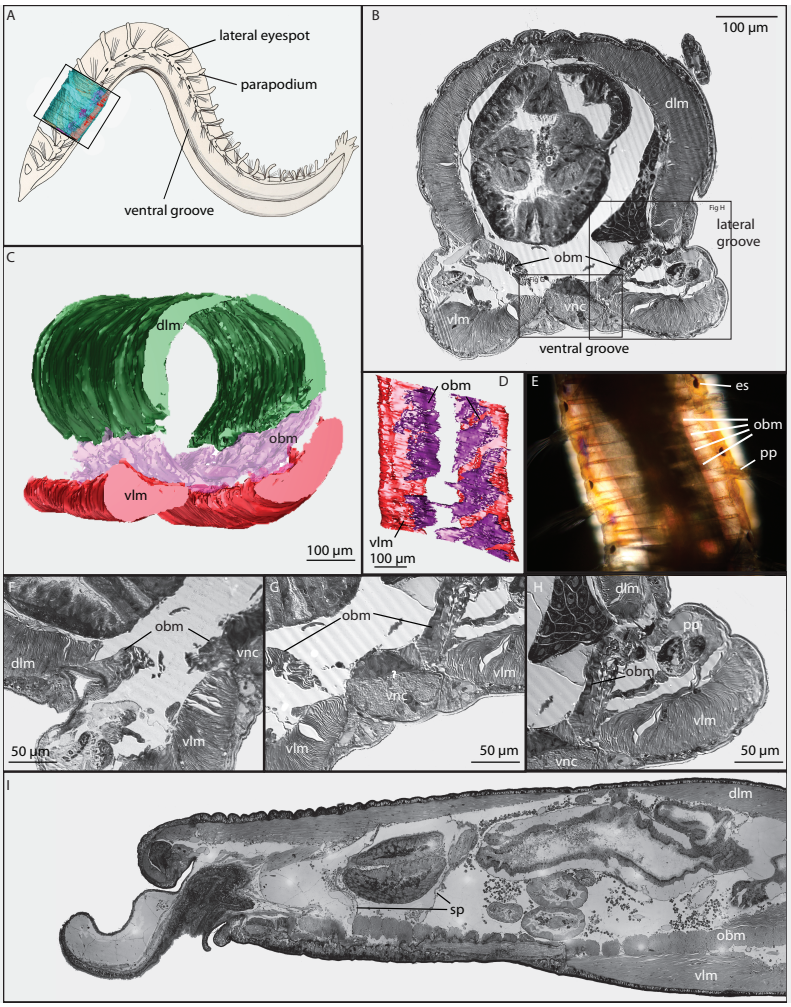

Fig. 4. Musculature of *Armandia brevis* (**A**) Schematic drawing of *Armandia brevis* (lateral view). (**B**) 1.5-µm semithin cross section. (**C**) 3D-reconstruction of body musculature over four anterior segments excluding the head (front-lateral view). (**D**) 3D-reconstruction of oblique muscles and ventral longitudinal muscles, shown in dorsal view. (**E**) Polarized image of ventral view of the body, revealing four bands of oblique muscle per segment; segments distinguished by eyespots and parapodia. (**F**) Semithin cross section, oblique muscle attaching to the epidermis (between parapodia). (**G**) Semithin cross section, oblique muscles attaching dorsal to the ventral nerve cord. (**H**) Semithin cross section, oblique muscle attaching to epidermis dorsal to parapodium. (**I**) Longitudinal cross section revealing two anterior septa. dlm, dorsal longitudinal muscles; es, eyespots; g, gut; obm, oblique muscles; pp, parapodia; sp, septa; vlm, ventral longitudinal muscles; vnc, ventral nerve cord. To activate the interactive 3D mode, view PDF in Adobe Reader and click on the image plate.

muscles; dorsal longitudinal muscles become thinner middorsally but are not completely divided. The posterior region of the body has musculature similar to *A. brevis*, with longitudinal muscle bands directly beneath the epidermis and no circular muscles in between. Oblique muscles extend from the ventral nerve cord to the lateral epidermis between the dorsal and ventral longitudinal muscles (Fig. 6J–N). The oblique muscles attach more ventrally than those of *A. brevis* (Fig. 4B), below the ventral nerve cord (Fig. 6J). In addition, in *T. mucronata*, a secondary, more ventral band of oblique muscle extends from the body wall ventral of the ventral nerve cord to either the lateral epidermis or the parapodial muscle complex (Fig. 6K,L). Longitudinal muscle bands are much smaller (Fig. 6J) than those of *A. brevis* (Fig 4B).

In the head, chaetigers, thorax, and lateral ridges of the anterior region, a thin, nearly continuous layer of circular muscle lies beneath the epidermis (Fig. 6B–G). Circular muscle is also found in the transitional region between the thorax and abdomen, becoming less continuous more posteriorly: circular muscle gradually disappears ventrally in Chaetiger 9 of the thorax and becomes completely absent ventrally in Chaetiger 10 (Fig. 6F,H). Circular muscles are present dorsally (Fig. 6F,G) and in the lateral ridge (Fig. 6I) until the transitional Chaetiger 11 (Fig. 6J,M). Oblique muscles are also found in the anterior region of

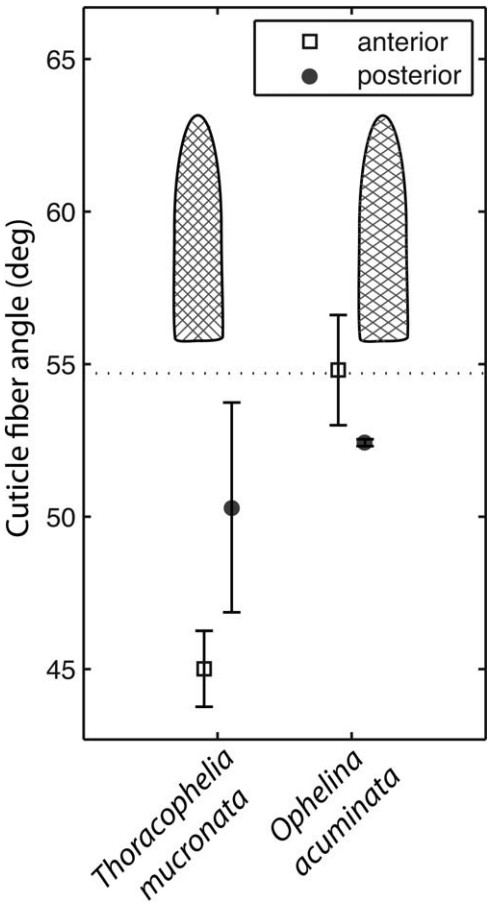

Fig. 5. Cuticle fiber angle (mean ± s.d.) of the anterior and posterior of *Thoracophelia mucronata* ($n = 8$) and *Ophelina acuminata* ($n = 4$). A dotted line is drawn at 54° 44'. Schematic of anterior fiber angles shown for each species to illustrate differences.

the body, first apparent anterior to the septum in Chaetiger 3 (cf. Fig. 8). Anterior oblique muscles connect dorsal and ventral circular muscles, attaching lateral to the ventral nerve cord, and are much thinner than in the posterior (Fig. 6B–F). Circular muscle in the anterior region bifurcates on both sides of the ventral nerve cord, with one branch extending away from the body wall to form oblique muscle (Fig. 6B,D,F,H). These oblique bands extend lateral-dorsally through the body cavity and reconverge with circular muscle in the lateral body wall between the epidermis and dorsal longitudinal muscles (Fig. 6B,C,F,G). Gaps in the longitudinal muscle, both ventrally and laterally, allow oblique muscle to branch from circular muscle (which lies between the longitudinal muscle, where present, and the epidermis) into the coelomic cavity (Fig. 6).

A single muscular septum separates the anterior of body cavity between the third and fourth chaetigers of the thorax (Fig. 8A). The septum encapsulates the pharynx and extends over the esophagus to form the "injector organ" that in this specimen extends from the 6th to 9th chaetigers. The septum separates the head from the main body cavity (Fig. 8). The septum/injector organ complex also consists of septal longitudinal and circular muscle fibers (Fig. 8C,E,G).

Cuticle fiber angles were not significantly different between the two methods of anesthetizing *T. mucronata*, with $MgCl_2$ before fixation in glutaraldehyde ($n = 3$) and with cold, placing worms in the freezer without fixation ($n = 5$; ANOVA, $P > 0.05$). Results were therefore combined ($n = 8$). Fiber angles in both the thorax and abdomen were < 54° 44′ (t-test, $P < 0.01$), with anterior fiber angles significantly smaller than posterior (ANOVA multiple comparison test, $P < 0.05$; Fig. 5). Thoracic fiber angles were significantly smaller for *T. mucronata* than *O. acuminata* (ANOVA multiple comparison test, $P < 0.01$), but abdominal fiber angles were not significantly different between the two species (ANOVA multiple comparison test, $P > 0.05$).

Functional Morphology of the Anterior of *T. mucronata* during Peristaltic Burrowing

Direct peristaltic movement in *T. mucronata* involves not only anteriorly-traveling waves of contraction of circular and longitudinal body wall muscles, but considerable movement of the septum, injector organ, and coelomic fluid (Fig. 9; Supporting Information, S-Movie). As the peristaltic wave moves forward into the head region, contraction of body wall circular and longitudinal muscles and relaxation of the septum pushes the pharynx backwards and forces coelomic fluids from the head region into the injector organ (Fig. 9A–E). Subsequent contraction of the septal circular and longitudinal muscles forces the pharynx and coelomic fluid back into the head region, expanding the head radially (Fig. 9F–J).

Phylogenetic Analyses

The maximum parsimony (MP) and maximum likelihood (ML) analyses for the combined molecular data produced similar results, though the ML topology is shown here (Fig. 10). There were differences in the placement of *Arenicola* between the two analyses (see below), and there were two most parsimonious trees of length 4652 steps that only differed from each other in the placement of *Ophelia. rathkei* and *O. bicornis*. Monophyly of Opheliidae was well supported (ML bootstrapping = BS: 100%; MP jackknifing = JK: 100%), as were the two subfamilies Opheliinae and Ophelininae. However, paraphyly was found for several genera and for one species-level taxon. Within Ophelininae, *Ophelina* was paraphyletic. The specimens of *O. acuminata* formed a clade that was the sister group to a well-supported clade comprised of the remaining ophelinins. The two specimens identified as *O. cylindricaudata (*New England, USA

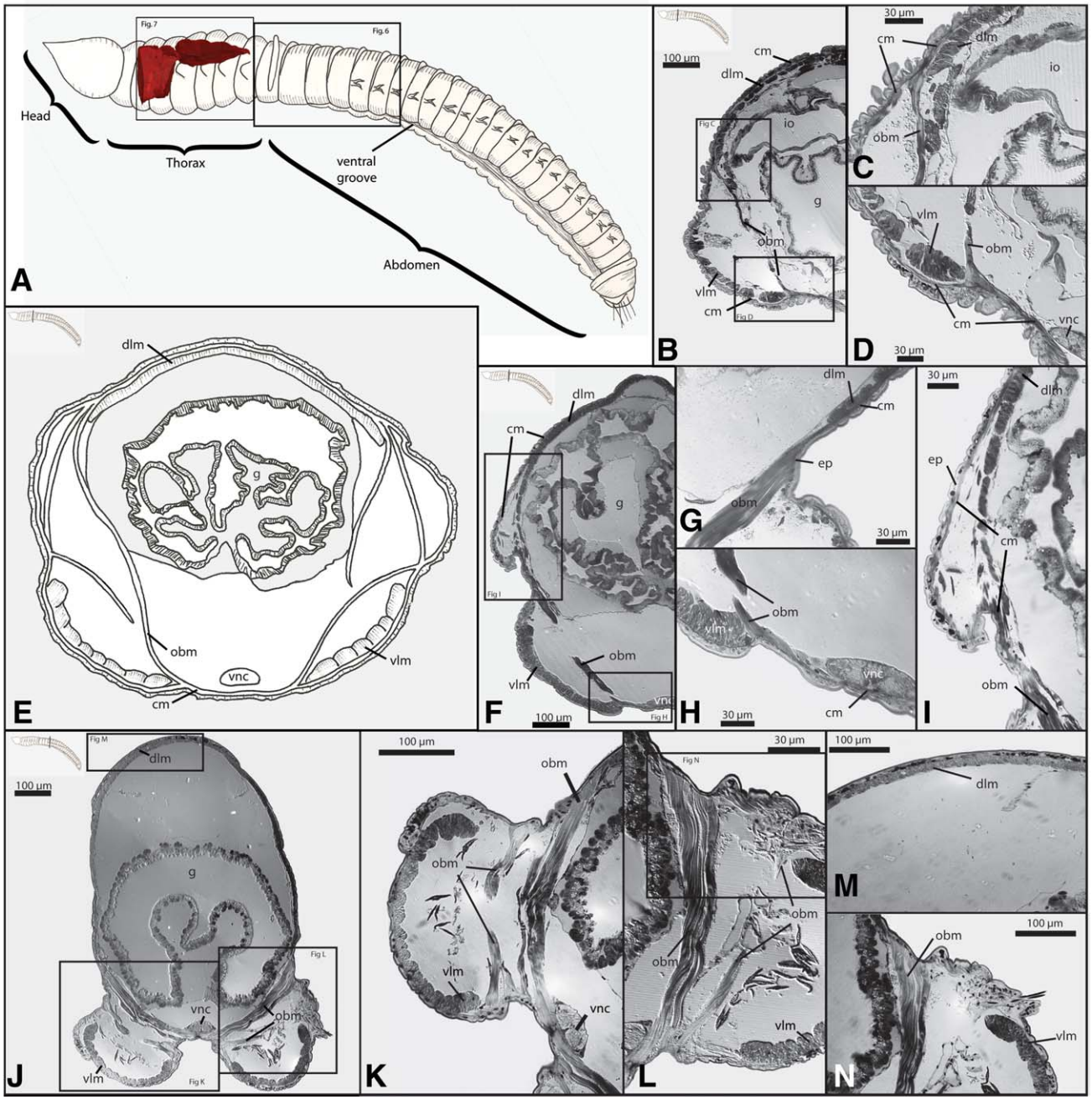

Fig. 6. Musculature of *Thoracophelia mucronata* (**A**) Schematic drawing of *Thoracophelia mucronata* with septum/injector organ shown in red (lateral view). (**B**) Semithin cross section of Segment 8. (**C**) Close up from B (lateral-dorsal). Band of oblique muscles (obm) merge with a continuous band of circular muscles (cm) between the epidermis and dorsal longitudinal muscles (dlm). (**D**) Close up from B (lateral-ventral). Thin layer of circular muscles lies between the epidermis and ventral longitudinal muscles (vlm), merging with a band of oblique muscles that continues dorsally. (**E**) Schematic drawing of a cross section (thorax region) showing the general pattern of oblique muscles and circular muscles. Circular muscles underlie the epidermis and bands of oblique muscles connect circular fibers ventrally, laterally, and dorsally. (**F**) Semithin cross section of Segment 10. No circular fibers present between epidermis and vlm. Dorsal and ventral circular muscles are connected by oblique muscle. (**G**) Close up of the right side of the section shown in F (lateral). Band of circular muscles between the epidermis and dorsal longitudinal muscles (dlm) extend away from the body wall and thicken to form oblique muscles (obm). (**H**) Close up from F (ventral). Band of oblique muscle merges with circular fibers between ventral nerve cord and epidermis. No circular fibers are present between epidermis and vlm. (**I**) Close up of lateral ridge from F (lateral). Circular muscle fibers are visible beneath the epidermis of the lateral ridge. (**J**) Semithin cross section of Segment 14. (**K**) Close up of nonparapodial side from J (ventral). Circular muscle fibers are absent, and multiple oblique muscle bands attach to epidermis. (**L**) Close up of parapodial side from J (ventral). Oblique muscle bands attach to epidermis. Secondary oblique muscle bands attach to parapodial complex. (**M**) Close up from J (dorsal). No circular fibers present between dlm and epidermis. (**N**) Close up from L (ventral). No circular fibers present between vlm and epidermis. dlm, dorsal longitudinal muscles; ep, epidermis; g, gut; io, injector organ; obm, oblique muscles; vlm, ventral longitudinal muscles; vnc, ventral nerve cord.

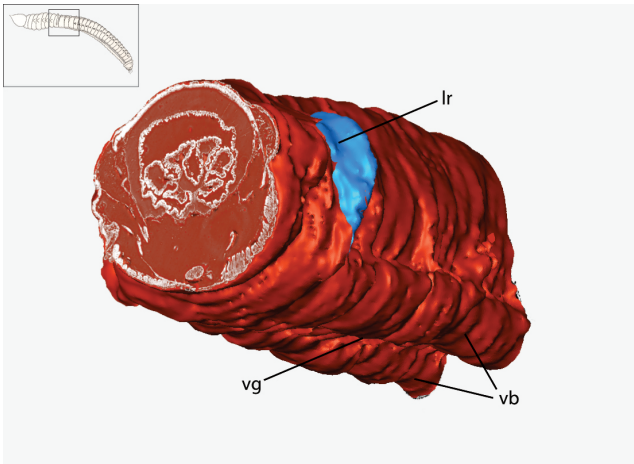

Fig. 7. 3D-reconstruction of Chaetigers 9–14 in *Thoracophelia mucronata*, showing the external morphological transition from thorax to abdomen (front-lateral view). lr, lateral ridge; vb, ventral bundle; vg, ventral groove. To activate the interactive 3D-mode, view PDF in Adobe Reader and click on the image plate.

and western Greenland) did not form a clade, with several specimens of unidentified *Ophelina* (from the eastern Pacific Ocean; Oregon and Costa Rica) forming a clade with the Greenland specimen of *O. cylindricaudata*. *Ophelina* was further found to be paraphyletic in that *Ophelina* sp. 1 (from the western Atlantic Ocean; North Carolina) formed a well-supported clade with *Armandia* and *Polyophthalmus*. *Armandia* was also found to be paraphyletic, with *Polyopthalmus* well nested inside this group. Within Opheliinae, *Ophelia* was paraphyletic with *O. limacina* recovered as the sister group to *Thoracophelia* under ML, rather than grouping with the other *Ophelia* specimens, though with poor support. In contrast, the MP analysis showed *Thoracophelia* to be paraphyletic with respect to *Ophelia* (not shown), also with poor support.

Our data supported a clade comprising Opheliidae and *Polygordius*, though with very low support under ML, in contrast to the strong support under MP (BS 46; JK 99). Scalibregmatidae was found to be sister to Opheliidae/*Polygordius* under MP (not shown), with strong support (JK 99), though under ML *Arenicola* was the sister-group to Scalibregmatidae (Fig. 10), albeit with low support. The monophyly of Scalibregmatidae, including *Travisia*, was well supported (BS 91; JK 100). *Travisia* formed a clade with *Neolipobranchius*, and this clade is sister to the remaining scalibregmatids.

Character Transformations

For characters with multiple most parsimonious reconstructions (MPRs), only two of the possible reconstructions were used: using an accelerated transformation (ACCTRAN), where changes are assigned as close to the root as possible and reversals are favored, and a delayed transformation (DELTRAN), where changes are assigned as far away from the roots as possible and convergence is favored. The ML tree topology shown in Figure 10 was used for the transformations.

Burrowing mode (Character 1) showed two MPRs. Both showed that peristaltic burrowing is a plesiomorphic for the ingroup (Fig. 11A), and under ACCTRAN there was a transition from peristaltic to undulatory burrowing for the Opheliidae/*Polygordius* clade, with a subsequent reversal back to peristaltic burrowing for Opheliinae (Fig. 11A). Under DELTRAN, peristaltic burrowing was the plesiomorphic condition for Opheliidae with undulatory burrowing appearing twice, once for *Polygordius* and once for Opheliininae. This ambiguity is complicated by the poor support for the clade comprising *Polygordius* as sister to Opheliidae. Of our sampled taxa, only *Notomastus* was scored with retrograde peristalsis (Character 2). The change from retrograde to direct peristalsis therefore occurred either below or at the ingroup node, and thus it is unclear as to whether retrograde peristalsis or direct peristalsis is the plesiomorphic condition for our terminal taxa. Direct peristalsis was, however, shared among Scalibregmatidae, *Arenicola*, and Opheliidae.

Only the terminals *Notomastus* and *Arenicola* were scored with proboscis use during burrowing (Character 3), which consisted of five MPRs. Under ACCTRAN, loss of proboscis use occurred once for the ingroup, with a subsequent reappearance in *Arenicola*. Under DELTRAN, a loss of proboscis use appeared independently for the scalibregmatid clade and also the Opheliidae/*Polygordius* clade. Various MPRs occurred owing to the unknown states for many of the scalibregmatid and *Travisia* terminals.

The multistate character pertaining to circular musculature (Character 4) consisted of seven MPR (Fig. 11B). Under ACCTRAN, circular muscle bands were lost in the Opheliidae/*Polygordius* clade, with a reappearance of circular muscles in *P. appendiculatus* and a second reappearance, restricted to the anterior region of the body, in Opheliinae. Under DELTRAN, loss of circular muscles appeared independently in the Opheliininae clade and in *P. lacteus*. In addition, the loss of circular muscles in the posterior region appeared in the Opheliininae clade. There were three MPRs for the character based on oblique musculature (Character 5). Under ACCTRAN, the presence of oblique muscles appeared at the ingroup node with a subsequent loss in *Arenicola* whereas, under DELTRAN, oblique muscles appeared independently in Scalibregmatidae and the Opheliidae/*Polygordius* clade.

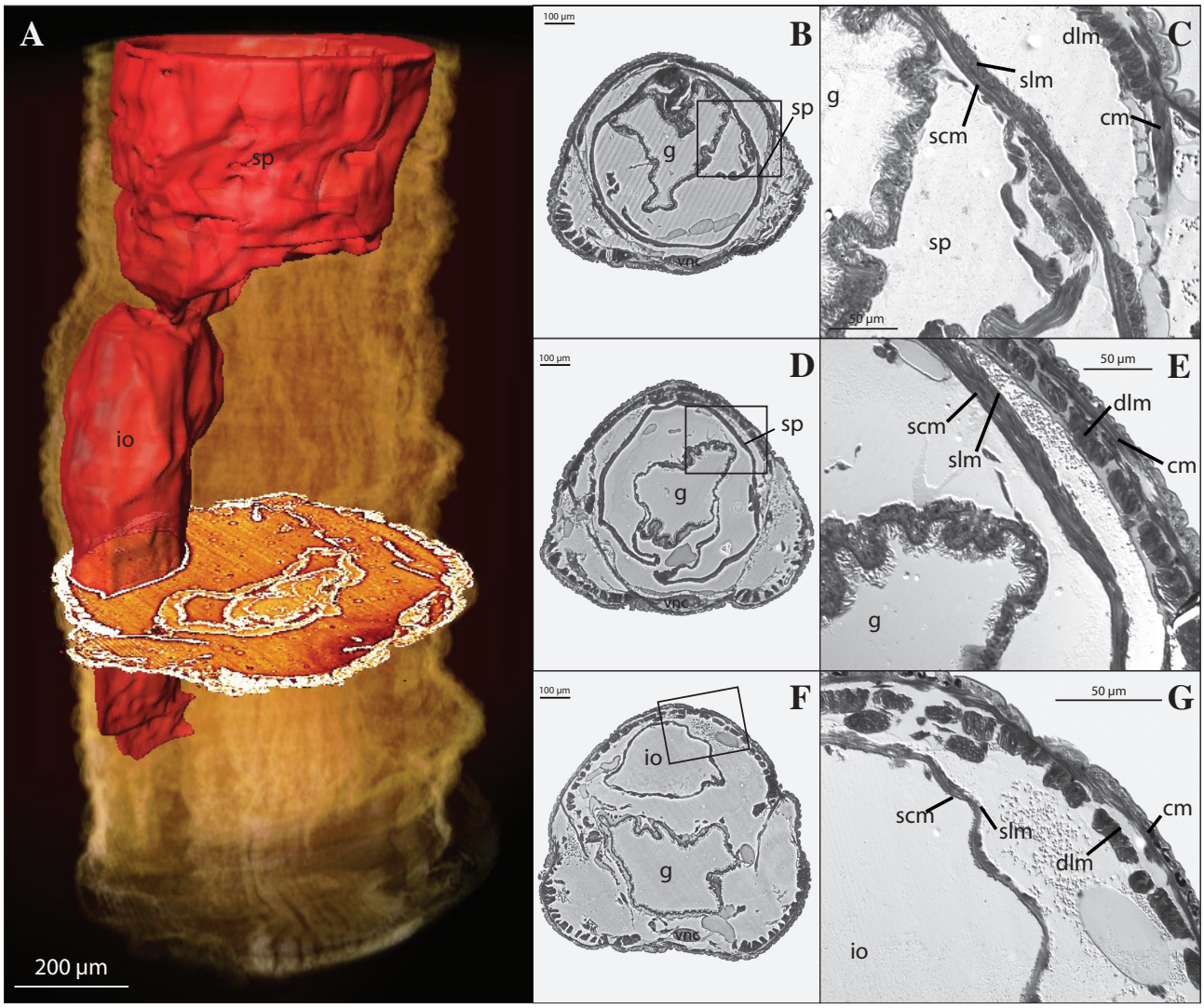

Fig. 8. Septum and injector organ of *Thoracophelia mucronata* (**A**) 3D-reconstruction of septum and injector organ (lateral view). (**B**) Semithin cross section from segment 4. (**C**) Close up of B showing septum with septal longitudinal and septal circular muscles. (**D**) Semithin cross section from segment 6. (**E**) Close up of D showing septum/injector organ transition with septal longitudinal and circular muscles. (**F**) Semithin cross section from segment 8. (**G**) Close up of F showing injector organ with septal longitudinal and circular muscles. cm, circular muscles; dlm, dorsal longitudinal muscles; g, gut; io, injector organ; slm, septa longitudinal muscles; sp, septum; scm, septal circular muscles. To activate the interactive 3D-mode, view PDF in Adobe Reader and click on the image plate.

The multistate character pertaining to septa (Character 6) only consisted of one MPR (Fig. 11C). Of the ingroup taxa, only *Polygordius* exhibited the outgroup condition of septa along the entire body. Loss of body septa along the body occurred twice, once for the clade of scalibregmatids and *Arenicola* and once for Opheliidae. *Notomastus*, *Arenicola*, and the opheliid subfamily Opheliinae were scored with the presence of modified anterior septa (Character 7), which resulted in eleven MPRs, owing to the large number of terminals with unknown states. Under ACCTRAN, appearance of one or more altered anterior septa occurred once for the ingroup, with a subsequent disappearance in Scalibregmatidae, *Polygordius*, and Opheliininae. Under DELTRAN, 1 or more altered anterior septa appeared independently in *Notomastus*, *Arenicola*, and Opheliinae.

Habitat distribution (Character 8) showed eight MPRs. Under ACCTRAN, a shift from mud-dwelling to sand-dwelling occurred at the ingroup node, with mud-dwelling reappearing twice, in Scalibregmatidae and in the opheliid subfamily Opheliininae (Fig. 11D). Sand-dwelling secondarily reappeared in *Armandia bilobata* and in the *Polyophthalmus* clade along with a subsequent secondary reappearance of mud-dwelling in *A. brevis* (Fig. 11D). Alternatively, five independent changes from mud-dwelling to sand-dwelling occurred under DELTRAN: once in *Arenicola*, once in

Polygordiidae, once in the opheliid subfamily Opheliinae, once in *A. bilobata*, and once in the *Polyophthalmus* clade.

The multistate character pertaining to ventral groove (Character 9) consisted of one MPR (Fig. 12A). The transformation shows a ventral groove along the whole body as plesiomorphic for the Opheliidae/*Polygordius* clade before transforming to being restricted to the posterior end in Opheliinae. The presence of a ventral groove restricted to the posterior end also appeared independently in *Scalibregma* (Fig. 12A). The presence of a ventral groove has been attributed to attachment of oblique muscles (Clark and Hermans, 1976), and the MPR for oblique muscles corresponds well to that of the presence of a ventral groove (data not shown). The ventral groove MPR also showed some interesting congruence with the MPR for the circular muscle character (Fig. 12B). The absence or restriction of circular muscles was coincident with presence of a ventral groove in the Opheliidae/*Polygordius* clade. The exception was the ventral groove (restricted to the posterior end) found in *Scalibregma* where circular muscles are present along the body.

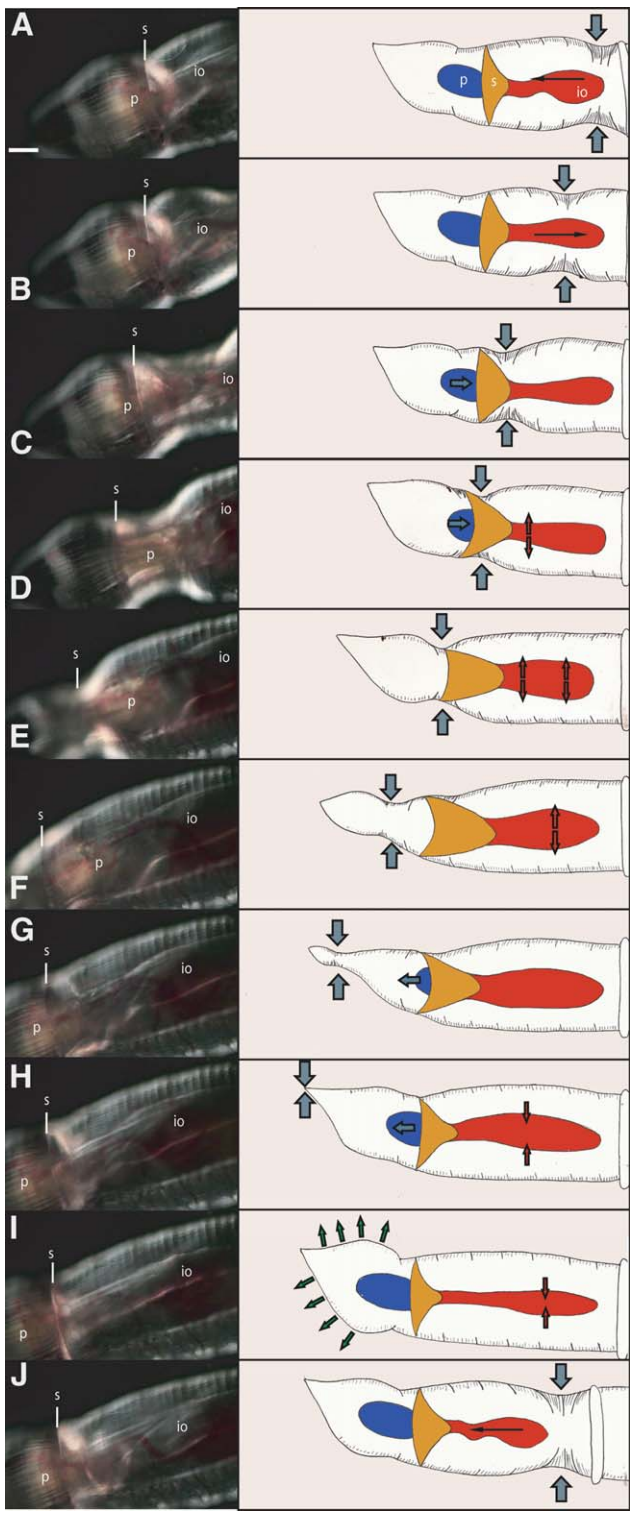

Fig. 9. Images with schematic drawings of the burrowing mechanism in *T. mucronata*. (**A**) Relaxed anterior showing septum (s) in gold in the drawing, pharynx (p) drawn in blue, and injector organ (io) drawn in red. Scale bar = 200 μm (all images at same scale). (**B**) 0.27 s, peristaltic wave moving anteriorly. (**C**) 0.6 s, peristaltic wave approaches septum. (**D**) 0.9 s, peristaltic wave close to septum contact with body wall, pharynx moving posteriorly, septum relaxed and extending, injector organ inflating. (**E**) 1.23 s, peristaltic wave moving anterior of septum, septum-body wall contact moving forward, pharynx posterior of septum-body wall contact, septum relaxed, injector organ inflated. (**F**) 1.63 s, head moving forward, septum-body wall contact moved forward, pharynx still posterior of septum contact but moving forward, injector organ inflated. (**G**) 1.87 s, pharynx moving forward and septum muscles contracting, injector organ muscles starting to contract, anterior close to or at full distance travelled. (**H**) 2.0 s, Septum mostly contracted, pharynx anterior of septum contact, injector organ contracting, anterior has reached full distance travelled. (**I**) 2.47 s, Septum fully contracted, head fully expanded, injector organ fully contracted. (**J**) 3.03 s, Septum and injector organ relaxed, injector organ partially inflated.

DISCUSSION

Functional Morphology of Undulatory Burrowing in *A. brevis*

Undulating movements of *A. brevis* resemble those of nematodes both in qualitative behavior and in body shape, characterized by the ratio of amplitude to wavelength (Dorgan et al., 2013). Like nematodes, *A. brevis* has thick bands of longitudinal muscle that contract unilaterally for undulatory bending. Bending during undulatory burrowing requires unilateral contraction of longitudinal muscles simultaneously with a mechanism to resist radial expansion and axial shortening on the side of muscle contraction. As the wave of contraction passes posteriorly, longitudinal muscles on the nonbending side contract, extending the contracted longitudinal muscles and serving as a

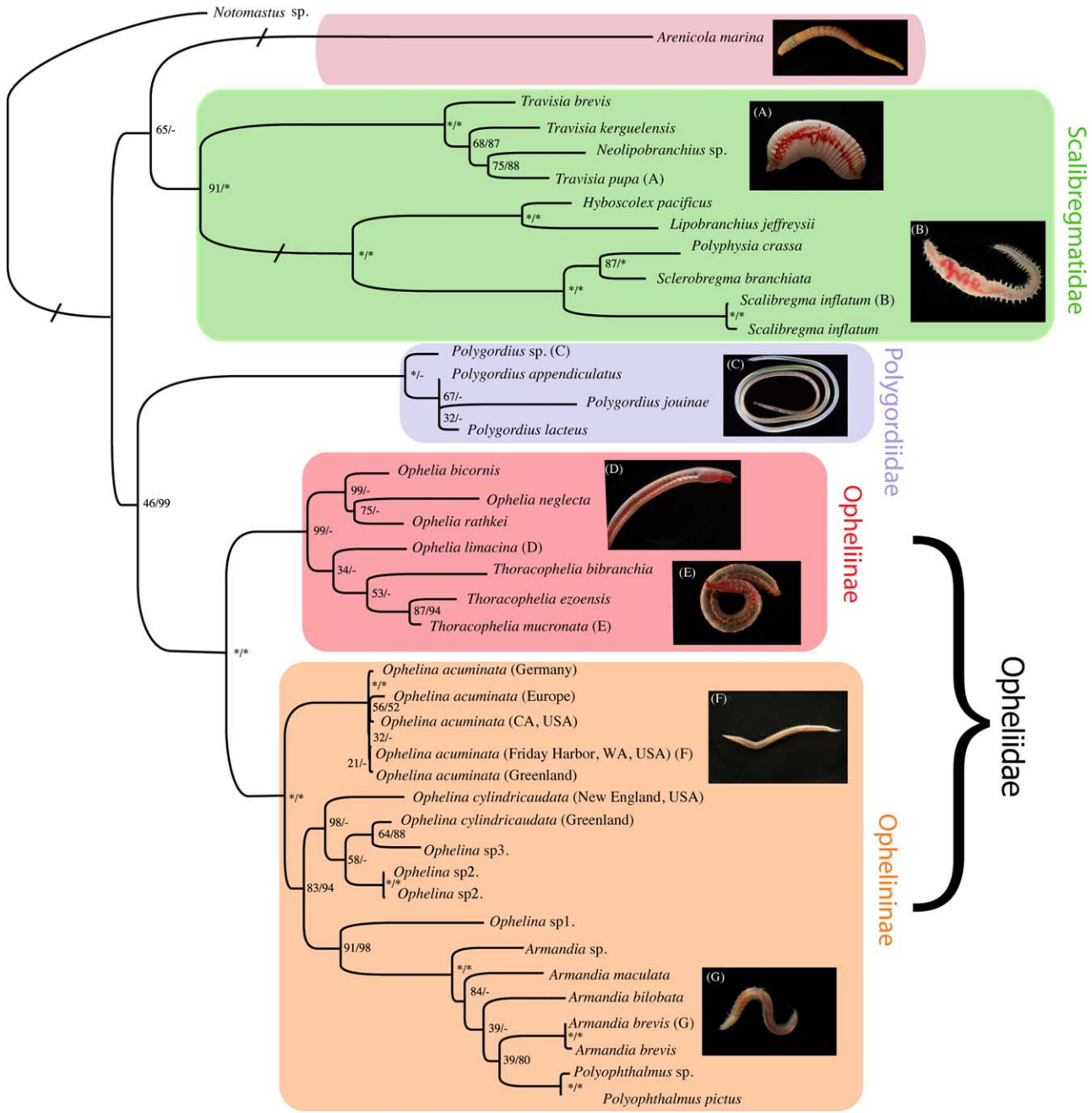

Fig. 10. Phylogenetic results of maximum likelihood tree from combined molecular data. Support values are shown as bootstrap from maximum likelihood and jackknife from maximum parsimony analyses, respectively, separated by /. * indicates 100% bootstrap support.

restoring force. The contracted oblique muscles presumably also extend when the body reaches the opposite curvature, although contraction of the ventral longitudinal muscle would likely extend relaxed oblique muscles as well. In the nematode *A. lumbricoides*, radially-oriented cuticle fibers prevent unilateral radial expansion, enabling longitudinal muscle contraction to bend the body (Fig. 1C). We found that helical fibers in the cuticle of *O. acuminata*, a closely related species to *A. brevis* with very similar undulatory behavior and morphological and muscular features (Law and Dorgan, unpublished data), have fiber angles much lower than that of *A. lumbricoides*, consistent with findings by Clark and Hermans (1976). This suggests that the cuticle of *A. brevis* does not resist radial expansion in the same way as that of *A. lumbricoides*, rather that the oblique muscles contract on the same side as the longitudinal muscles to enable bending (Fig. 13).

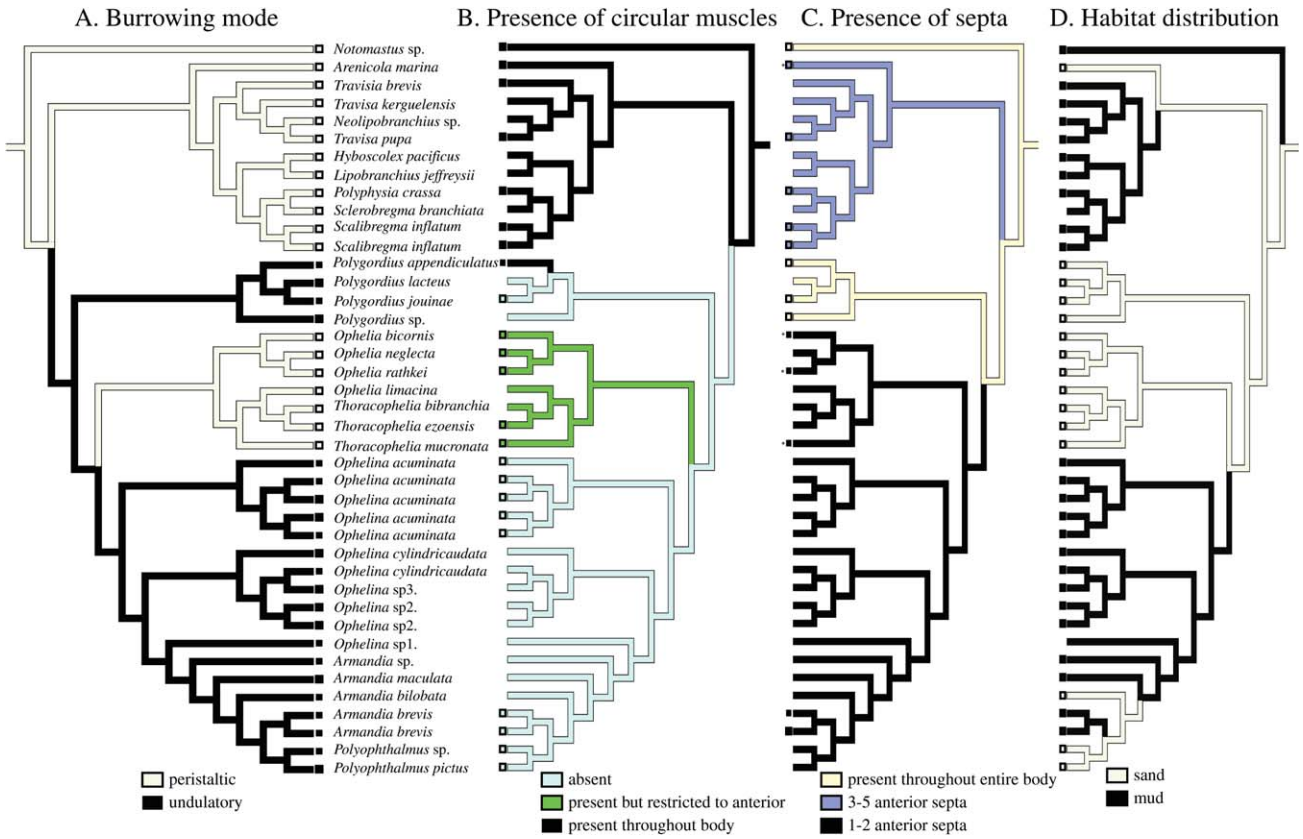

Fig. 11. Character transformations using parsimony reconstruction methods. Tree topologies identical to tree seen in Figure 9. (**A**) Burrowing mode. (**B**) Presence of circular muscles. (**C**) Presence of septa. * indicates modified anterior septum. (**D**) Sand/mud habitat distribution.

Helical fibers not only resist expansion or elongation depending on their angle, but they also control the maximum volume in a cylinder and the extent to which body shape can change. At an intermediate fiber angle of 54° 44′, a cylinder reaches its maximum volume, and, if turgid, the fibers will resist both expansion and elongation (Kier, 2012). The cuticle fiber angle in *O. acuminata* is not significantly different from 54° 44′, corresponding to the maximum volume of a circular cylinder, consistent with observations of rigid-bodied live worms. The cuticle, therefore, appears to function to prevent both radial expansion and axial elongation and may facilitate both bending and axial forcing against the substratum during forward movement.

Functional Morphology of Peristaltic Burrowing in *T. mucronata*

Peristalsis in burrowers with segments separated by muscular septa, such as the earthworm *Lumbricus terrestris*, is described as a nearly simultaneous wave of circular and longitudinal muscle contractions of the body wall traveling in the opposite direction of locomotion (Gray and Lissmann, 1938; Clark, 1964). For direct peristalsis, in which waves of contraction of the body wall travel in the direction of movement to result in forward movement, fluid must be able to travel away from the region of contraction and thus requires an open body cavity (Clark, 1964; Elder, 1980). *T. mucronata* has an open body cavity consistent with direct peristalsis, but we show that activity of muscles of the septum and injector organ accompany anteriorly-traveling waves of contraction of circular and longitudinal muscles in the body wall. Muscle contractions in the septum/injector organ complex force coelomic fluid into the head region following passage of the peristaltic wave along the body wall (Fig. 9). This expansion of the anterior is likely important both in burrow construction and in anchoring to allow the remaining posterior body to be pulled forward into the burrow. Analogous structures for anterior expansion are found in other direct peristaltic burrowers as well: *Arenicola marina* has a modified anterior septum, the gular membrane, that is important in pharynx eversion (Wells, 1954), and the priapulid *Priapulus caudatus* has an open body cavity but

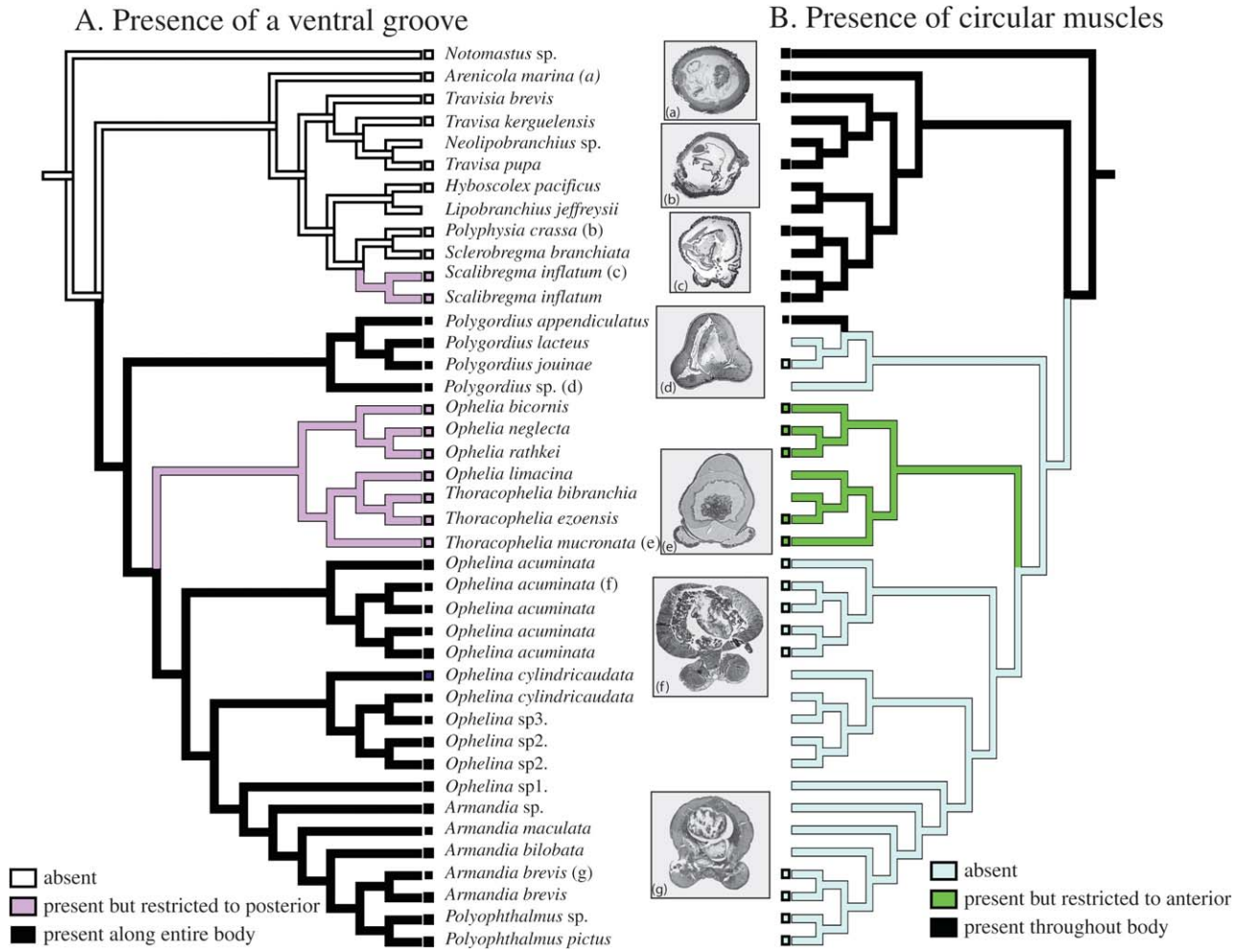

Fig. 12. Character transformations using parsimony reconstruction methods. Tree topologies identical to tree seen in Figure 9. (**A**) Presence of ventral groove. (**B**) Presence of circular muscles.

uses an eversible praesoma to expand the anterior (Elder and Hunter, 1980).

The difference in angle of helical fibers in the cuticle between *T. mucronata* and *O. acuminata* is consistent with their different locomotory behaviors. More axially-oriented fibers in the anterior of *T. mucronata* resist axial elongation of the anterior so that an increase in internal pressure causes radial expansion (Clark and Cowey, 1958). The lower cuticle fiber angle indicates that the volume of fluid is less than the maximum, consistent with observations of a less turgid body in *T. mucronata* than in *A. brevis* and *O. acuminata* (cf. Clark and Cowey, 1958). Cuticle fiber angles are not significantly different in the posterior of the two species, which has more similar musculature as well.

As with other members of Opheliinae (e.g., *Ophelia rathkei*; Brown, 1938), the posterior region of *T. mucronata* resembles the body plan of *A. brevis* in lacking circular muscle (Fig. 6J–N). However, compared to the thick and robust musculature of *A. brevis*, both longitudinal and oblique muscles in *T. mucronata* appear much thinner (Fig. 4B,6J). Whereas undulations occur along the entire length of *A. brevis*, the posterior of *T. mucronata* is much less active during burrowing. Rather than simply being dragged passively behind the anterior however, the posterior appears to be pulled along in discrete anterior movements (Dorgan, unpublished data), presumably by simultaneous contraction of longitudinal muscles on both sides of the body. Rather than having a single thick band of oblique muscle as in *A. brevis*, *T. mucronata* has two thinner bands, with a more ventral second band that attaches laterally at the parapodia or just ventral of the lateral groove (Fig. 6M,N). We suggest that this secondary muscle band may both assist in parapodial control and also enable greater control of changes in body shape around the ventral ridge. Observations of live worms show considerable anterior-posterior movement of coelomic fluid through the ventral

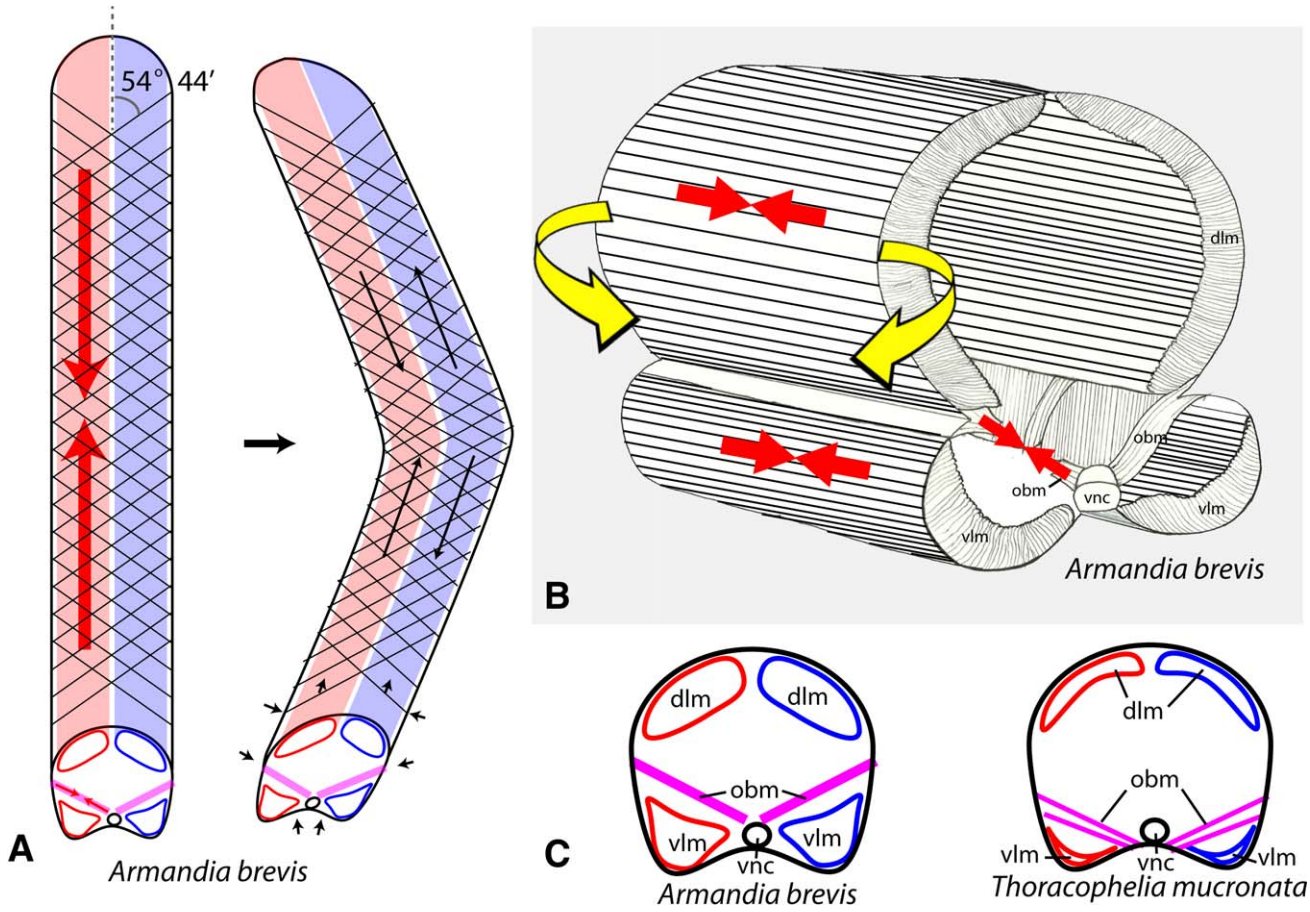

Fig. 13. Schematic drawing of musculature used for bending in *Armandia brevis* and *Ophelina acuminata* from frontal dorsal (**A**) and frontal lateral (**B**) views. Bending (yellow arrows) is achieved by the unilateral contraction of dorsal and ventral longitudinal muscles (red arrows) simultaneously with the antagonistic contraction of oblique muscles on the same side (red arrows). Contraction of oblique muscles acts to resist radial expansion and axial shortening, and longitudinal muscles on the opposite side serves as the restoring force. Inextensible helical fibers in the cuticle are oriented at an intermediate fiber angle (between radially and axially oriented) corresponding to the maximum volume of a circular cylinder and may help prevent radial expansion as well as axial elongation (black arrows). (**C**) Schematic of cross-section of *Thoracophelia mucronata* shown for comparison. Oblique muscles attach below the ventral nerve cord, a position likely to be less effective in resisting radial expansion. dlm, dorsal longitudinal muscles; obm, oblique muscles; vlm, ventral longitudinal muscles; vnc, ventral nerve cord.

ridges on either side of the ventral groove. Contraction of posterior oblique muscles may reduce the diameter of the body during forward movement, potentially reducing frictional resistance along the abdomen.

Phylogenetic Relationships

A. brevis and *T. mucronata* respectively belong in each of the two main clades within Opheliidae; the former in the undulatory Opheliininae and the latter in the peristaltic Opheliinae. Although monophyly of the opheliid subfamilies was well supported, paraphyly of genera was found within both subfamilies. Although a clade of two specimens of *Ophelina cylindricaudata*, two specimens of *Ophelina* sp. 2, and a single specimen of *Ophelina* sp. 3 was recovered, they likely belong to four different species (Fig. 10). In addition, *Ophelina* formed a grade, with *Ophelina* sp.1 forming a clade with *Armandia* and *Polyophthalmus* (Fig. 10). *Ophelina* sp.1 lacked the eyespots that occur in *Armandia* and *Polyophthalmus* and so was correctly assigned to this genus, though further assessment is clearly required. *Polyophthalmus* nested within a grade of *Armandia*. Whether *Armandia* Filippi, 1861 should be synonymized with *Polyophthalmus* Quatrefages, 1850 in future taxonomic revisions requires additional investigation. The absence of branchiae currently distinguishes *Polyophthalmus* from *Armandia* and *Ophelina* (Blake, 2000).

The MP and ML analyses showed incongruent topologies for the subfamily Opheliinae. The MP result showed *Ophelia* to be within a paraphyletic *Thoracophelia*, whereas ML (Fig. 10) showed *Ophelia* to be paraphyletic with respect to *Thoracophelia*. In each, the support for these topologies

was poor. The two genera have traditionally been distinguished by the difference in body regions: *Ophelia* has two distinct regions and *Thoracophelia* has three (Blake, 2000).

Similar morphological characteristics such as the presence of a ventral groove, undulatory burrowing behavior, and lack of circular muscles have linked polygordiids with opheliids such as *Armandia* and *Polyophthalmus* for over a century (McIntosh, 1875; Fraipont, 1887; Rouse and Pleijel, 2001). Our parsimony analysis did recover a clade consisting of Opheliidae and the morphologically similar *Polygordius* with strong support, though it was markedly lower with ML (Fig. 10), suggesting further investigation is required. Additionally, the only previous molecular-based analysis on a broader scale (Rousset et al. 2007) that included these taxa found no close relationship for Opheliidae and *Polygordius*. A recent phylogenetic study suggested that Scalibregmatidae and Opheliidae are sister groups (Paul et al., 2010), but this was not found by Persson and Pleijel (2005) or Rousset et al. (2007), and Struck et al. (2008) found that Scalibregmatidae was closer to *Fauveliopsis* and *Sternaspis* (neither included in our analysis) than to Opheliidae.

Our results showing that *Travisia* belongs with Scalibregmatidae, rather than Opheliidae, was consistent with findings first shown by Persson and Pleijel (2005) and then corroborated by Paul et al. (2010). The placement of *Travisia* into Scalibregmatidae confirms century-old discussions of morphological similarities between the two taxa and suggestions that there may have been problems with the placement of *Travisia* in Opheliidae (Ashworth, 1901; Blake, 2000; Rouse and Pleijel, 2001). Paul et al. (2010) found that their two species of *Travisia* formed a grade with respect to *Neolipobranchius*, suggesting that *Neolipobranchius* Hartman and Fauchald, 1971 should be synonymized with *Travisia* Johnston, 1840 in future taxonomic revisions. Our inclusion of a third species of *Travisia* (*T. kerguelensis*) also found that *Travisia* includes *Neolipobranchius*.

Evolution of Musculature

It has been well-documented that peristaltic burrowing behavior is common in polychaetes and involves both circular and longitudinal muscles (e.g. *Arenicola marina*, *Polyphysia crassa*, *L. terrestris*, *T. mucronata*; Trueman, 1966; Elder, 1973; Seymour, 1976). We found that the loss of circular muscles, in part of all of the body, coincided with a switch from peristaltic to undulatory burrowing in *Polygordius* (with the exception of *P. appendiculatus*; Lehmacher et al., in press) and some Opheliidae (Fig. 12A,B).

The reappearance of anterior circular musculature was found for Opheliinae, which are peristaltic burrowers. The presence of circular musculature anteriorly is consistent with our analysis showing that *T. mucronata* exhibits peristaltic movements in only the anterior region of the body, in contrast to other direct peristaltic burrowers for which the wave travels the entire length of the body (e.g., *P. crassa*; Elder, 1973).

The recent discovery of "minute" circular muscles in *P. appendiculatus* (Lehmacher et al., in press) is interesting as polygordiids exhibit undulatory behavior (Dorgan, unpublished data), whereas circular muscles are generally used in peristaltic burrowing. They also have oblique muscles, similar to *A. brevis*, which likely similarly act with unilateral contraction of longitudinal muscles to bend the body during undulation. It seems feasible that the circular muscles may act in conjunction with the oblique muscles to prevent radial expansion and enable bending, although their function during undulatory burrowing and whether circular musculature may occur in other polygordiids requires additional study.

With the exception of the outgroups *Notomastus* and *Arenicola*, all our terminal taxa (where known), both undulatory and peristaltic burrowers, showed oblique muscles that extend from the midventral line to the midlateral body wall. Oblique muscles either appear at the ingroup node, with a subsequent reversal in *Arenicola* (ACCTRAN), or appear independently in Scalibregmatidae and the Opheliidae/*Polygordius* clade (DELTRAN). Broader taxon sampling is needed to distinguish between these two alternatives. Better resolution of the position of *Polygordius* is particularly important in determining the evolution of undulatory burrowing among these taxa.

The function of oblique muscles appears to differ between undulatory and peristaltic burrowers. Oblique muscles are important during locomotion in *A. brevis*, acting with longitudinal muscles to achieve lateral bending (Fig. 13). The presence of similarly large oblique muscles as well as large longitudinal muscles in other undulatory *Ophelina*, *Polyophthalmus* (Purschke and Müller, 2006, Fig 2B), and *Polygordius* suggests similar mechanisms during undulatory behaviors. The oblique muscles of the peristaltic burrower, *T. mucronata* (Fig. 6K,L) occur as multiple thinner bands that attach at distinct positions along the body wall, and oblique muscles of the related *Ophelia* sp. appear to be similar (Brown, 1938). We suggest that these secondary muscle bands likely contract bilaterally rather than unilaterally as in *A. brevis* and may help contract the body to reduce friction as it is pulled forward with the longitudinal muscles.

The branching of circular muscles to form oblique muscles in the anterior of *T. mucronata* (Fig. 6C,D,G) suggests that oblique muscles may have been derived from circular muscles, although

our phylogeny leaves the plesiomorphic state of circular muscles in Opheliidae ambiguous, and we cannot discount the possibility that circular muscles may instead be derived from oblique muscles. This is further complicated by the poor support (ML) for a *Polygordius*/Opheliidae clade and by the presence of circular muscles in *P. appendiculatus* and uncertainty about other *Polygordius*. Transformations showing polygordiids lacking circular muscles (e.g., ACCTRAN), and the fact that oblique muscles are also shared by *Polygordius* and the Ophelininae clade, suggests that circular muscles may be secondarily derived from oblique muscles in *T. mucronata* and other Opheliinae (Fig. 12). An alternative MPR (DELTRAN), which showed polygordiids as having circular muscles, suggests that circular muscles were only lost once in Ophelininae. In this case, oblique muscles, present in the posterior of *Thoracophelia* and Scalibregmatidae, and presumably functioning to lift the ventral posterior and reduce friction as the posterior is dragged along, may have moved more proximally in *Armandia* to more effectively prevent radial expansion from longitudinal muscle contraction during bending. Further research on the development of musculature is needed to test this hypothesis.

Function of Septa in Burrowing

Of all our taxon terminals, only the outgroup taxon, *Notomastus*, and *Polygordius* spp. were scored with the presence of septa along the entire body (Fig. 12C). Scoring for *Polygordius* sp., *P. appendiculatus*, and *P. lacteus* was based on Fraipont's (1887) anatomical study of various polygordiid species in which he stated that the body cavity is separated by septa; presence of septa in *P. jouinae* remains unknown. Similarly, Rota and Carchini (1999) show the presence of intersegmental septa in the post oesophageal region based on serial sectioning of *Polygordius antarcticus*. Under the MPR shown in Figure 12C, body septa were lost twice, once in the clade of scalibregmatids and *Arenicola* and once for Opheliidae (Fig. 12C). Like earthworms, the fully septate *Notomastus* exhibits retrograde peristalsis (Dorgan, unpublished data). *Polygordius* exhibits undulatory rather than peristaltic movements (Clark and Hermans, 1976), similar to aseptate *Armandia*, but this is clearly not incompatible with the presence of septa along the body. *Polygordius* exhibits more complex movements than *Armandia*, and it is possible that septa may provide additional control for maneuvering through pore spaces in coarse sands and gripping grains to prevent being washed out of the sand.

With the exception of *Polygordius*, the majority of our ingroup taxa, both peristaltic and undulatory, have body cavities that are open and lacking septa, suggesting that an aseptate body form is not directly correlated with undulatory vs. peristaltic behavior. The function of anterior septa, however, does differ between the undulatory and peristaltic burrowers in our study. In the undulatory *A. brevis*, anterior septa are thin and not muscular. Anterior septa in *Armandia* likely function in anterior hydrostatic pressure changes necessary for proboscis eversion (Tzetlin and Zhadan, 2009). Unlike some muscular proboscises (e.g., nereids, glycerids), that of *A. brevis* is not used during burrowing (Dorgan et al., 2013). The anterior septum in *T. mucronata*, however, has both septal circular and longitudinal muscles that contract to inflate the head region and are synchronized with the direct peristaltic wave in the body wall (Fig. 9). Our anatomical analyses reveal that only one anterior septum/injector organ occurs in *T. mucronata*, which differs from the two anterior septa suggested by McConnaughey and Fox (1949). A possible explanation for McConnaughey and Fox's (1949) description of a second septum is that the oblique muscles, previously considered absent in the anterior region (Clark and Hermans, 1976), could easily be misinterpreted as a septum in serial sections (cf. Fig. 6).

Modified anterior septa also appear in other closely related opheliids. Previous studies on *Ophelia rathkei* by Brown (1938) and *O. bicornis* by Harris (1994) reveal that two anterior septa are present rather than just a single anterior septum as exhibited by *T. mucronata*. Each of the two septa gives rise to an injector organ, with one sac being inside the other (Fig. 14). Harris (1994) suggested that the injector organs are "passive," although still important in the maintenance of prostomial coelomic fluid pressure, as the walls of the injector organs in *O. bicornis* lacked contractile activity needed to inflate/deflate and push coelomic fluids from the organ into the head region. Rather, pressure created by the inflation of the blind capillaries of the prostomial plexuses against the inelastic cuticle provides additional turgidity during burrowing (Harris, 1994). Both the structure and function of the injector organ in *T. mucronata* differ from Harris' (1994) description of the injector organ in *O. bicornis*, with that of *Ophelia* appearing to be intermediate between the thin septa of *A. brevis* and the more muscular and extended injector organ of *T. mucronata*.

A modified anterior septum, termed a gular membrane, has also been described in *Arenicola* (Wells, 1954). Like in *T. mucronata*, a muscular anterior septum extends posteriorly to form the gular membrane, which regulates coelomic fluid pressure for proboscis eversion during burrowing and feeding (Wells, 1954; Dales, 1962; Trueman, 1966). The gular membrane and modified septum of *Thoracophelia* appear to be convergent, as other taxa included in our analysis, including

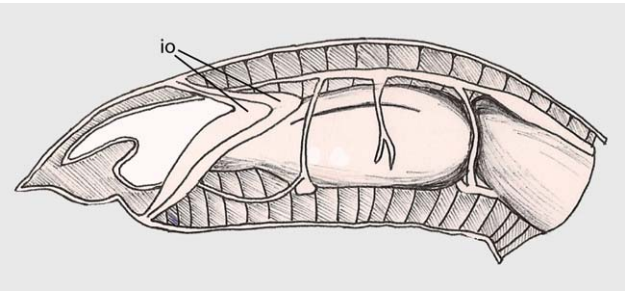

Fig. 14. Schematic drawing of the anterior of *Ophelia bicornis* showing two smaller injector organs (io) instead of just a single septum/injector organ as seen in *T. mucronata* (Fig. 7). Adapted from Harris (1994).

scalibregmatids, lack such modified septa. Scalibregmatids such as *Travisia pupa* and *S. inflatum* have three to –four anterior septa, the most anterior of which is relatively muscular (Dales, 1962). Dales (1962) suggests that these anterior septa help regulate fluid pressurization for proboscis eversion, which does not appear to be used by *S. inflatum* during burrowing (Dorgan, unpublished data).

Habitat Distribution

Even though the mechanical responses of muds and sands to burrowers are substantially different, muds are elastic materials through which most worms extend burrows by fracture, whereas sands are noncohesive granular materials, suggesting that morphologies and behaviors of burrowing animals might be distinct between these two habitats, our data showed that habitat distribution is variable and did not coincide well with burrowing mode, musculature, or presence of septa (Fig. 11). The nearly identical morphologies, musculature, and undulatory burrowing behavior within Opheliniinae did not coincide with a single sediment distribution: *A. bilobata* and *Polyophathalmus* are sand-dwelling whereas *Ophelina* and the remaining of our *Armandia* species are mud-dwelling. In muds, *A. brevis* does not extend burrows by fracture like most mud-burrowers. Rather its body undulations displace surficial aggregates of muddy sediment, a mechanism that seems just as feasible in surficial granular sands (Dorgan et al., 2013), perhaps explaining this range of habitats for morphologically similar species. However, even generalizations based on similar morphologies and musculature that appear to be convergent seem to be an unreliable indicator of habitat distribution. For instance, injector organs (or gular membranes) are found in *Arenicola* (Wells, 1954) and the *Thoracophelia*/*Ophelia* clade, suggesting that this convergent feature is an important characteristic for sand burrowing; however, the presence of a gular membrane in the mud-dwelling *Notomastus* (Eisig, 1887) does not follow this pattern. Moreover, *Thoracophelia* live in noncohesive, granular beach sands that differ mechanically from the heterogeneous sands in which arenicolids are found, where hydraulic fracture can result from irrigation, indicating that at least some of these sediments contain enough organic material to behave elastically (Matsui et al., 2011). Simple characterization of sand vs. mud may therefore overgeneralize the mechanical responses of sediments to burrowing behaviors. Similarities in musculature, lack of septa, and use of direct peristalsis by Scalibregmatidae and *Thoracophelia*/*Ophelia* suggest a similar function and potentially similar habitat, yet members of the former taxa inhabit muddy sediments, while the latter inhabit sandy beach environments. Linking habitat distribution to morphological characters is further complicated by the presence of both undulatory and peristaltic polychaetes in the same habitat (e.g., Woodin, 1974).

The high variability in habitat seen among our sampled taxa would increase further with greater taxonomic resolution. For example, whereas the four species of *Ophelia* included in this study are all found in clean sands, three species in that genus are found in muds or muddy sands (Bellan and Dauvin, 1991). Similarly, whereas most scalibregmatids are found in very fine muds, *Asclerocheilus beringianus* is found in sandy silts and *A. kudenovi* in the rocky intertidal (Blake, 2000), and species in the genera *Axiokebuita* and *Speleobregma*, not included in our analysis, crawl or swim through coarse gravel and boulders in caves (Martinez et al., in press). Future comparisons of habitat and morphological characters across a broader diversity of annelids are needed to determine whether these characters are correlated and may also identify additional convergence events.

External Morphologies

The ventral groove appears twice in the terminals assessed here; once in *S. inflatum* and once in the Opheliidae/*Polygordius* clade (Fig. 12A). This ventral groove is restricted to the posterior region of the body in Opheliinae and in *S. inflatum*. The presence of the ventral groove coincides well with the absence of circular muscles and the presence of oblique muscles: in the entire body of Opheliniinae and *Polygordius*, the ventral groove is present where circular muscles are absent and where oblique muscles are present, and in Opheliinae, the ventral groove is present only in posterior region of the body that also lacks circular muscles but contain oblique muscles. This trend is inconsistent in the peristaltic *S. inflatum*, where circular muscles remain present in posterior region despite being characterized by a ventral groove (Ashworth, 1901). The ventral groove is not as prominent as that of opheliids, however, and scalibregmids do have oblique muscles, contraction of

which has been suggested to form the ventral and lateral grooves (cf. Clark and Hermans, 1976). With the exception of some *Travisia*, e.g., *T. fusiformis*, *T. gravieri*, and *T. hobsonae* (Dauvin and Bellan, 1994), scalibregmatids have not been described as having a ventral groove. *S. inflatum* now represents the only other scalibregmatid to be scored with this feature, and whether other members of Scalibregmatidae have ventral grooves require additional anatomical study.

Interestingly, several other annelid taxa have ventral grooves, including Terebellidae (Nogueira et al. 2010), which are primarily tube-dwelling, suggesting that oblique muscles likely have a function more similar to those of *T. mucronata* than *A. brevis*. *Pisionidens* has oblique muscles that, like those of *Armandia*, extend diagonally across the coelomic cavity and create an externally visible groove, although in *Pisionidens* the oblique muscles connect dorsally rather than ventrally, resulting in a dorsal groove (cf. Fig. 2 of Tzetlin, 1987). *Pisionidens* lack circular muscles and live in sandy sediments, often interstitially, and their morphology indicates that they move similarly to *Armandia*. That oblique muscles appear to evolved independently in several independent clades and with clearly nonhomologous structures further supports their important role in locomotion.

CONCLUSIONS

Examination of the musculature of *A. brevis* and *T. mucronata* reveals a number of divergences that lend insight into the functional morphology of these two species. Our direct comparison identified several functionally important differences in morphologies, e.g., the attachment of oblique muscles, and the orientations of the helical fibers in the cuticle, in addition to previously described presence vs. absence of circular muscles. Variability in musculature that is closely tied to locomotory function is seen broadly across the taxa included in our phylogenetic analysis. Although most of our ingroup taxa lack septa all along the body and use direct peristalsis, the presence of septa in *Polygordius* suggest that even this feature is not consistent, but has been lost and regained even among this limited sampling of polychaetes. Both *Thoracophelia* and *Arenicola* have modified anterior septa that are important in burrowing, and these appear to be convergent features. Most of our characters show multiple equally parsimonious transformations, yet musculature seems to be closely tied to locomotory function and suggests that muscle structure is quite variable evolutionarily and that divergence of muscle structure may be key to evolving different behaviors. Supplementary investigation of the associated motor patterns, however, is required to fully understand the evolution of both muscular and functional change (Lauder, 1990). Habitat, characterized here as sand vs. mud, showed very poor phylogenetic consistency. This is unsurprising given the variability in musculature and that seemingly similar behaviors, e.g., direct peristalsis, are used by burrowers in both sands and muds.

Polychaetes are an abundant and morphologically diverse group of organisms and serve as important members of benthic communities (Rouse and Pleijel, 2001). Our results highlight the need for better understanding of both the locomotory functions of musculatures across a broader sampling of polychaetes and of the interactions between burrowing behaviors and habitat characteristics, for example, comparison of direct peristalsis in muds versus sands, in understanding the evolution of burrowing behaviors. Linking differences in morphologies between related taxa to their behaviors and habitats will give us greater context to the evolution and function of burrowing animals. Uncovering these functional roles allows better understanding of the relationship between community dynamics and ecosystem function as well as interpreting the importance of species diversity.

ACKNOWLEDGMENTS

GWR thanks Reinhardt Kristensen, Martin Sørensen, and Katrine Worsaae for the invitation to join the Arctic Workshop 2010: “Exploration of a cold trail: Arctic pieces to the puzzle of Evolution” and the Board of the Arctic Station for logistical support. Special thanks to José Ignacio Carvajal for assistance with DNA sequencing, Harim Cha for accessioning the vouchers into the Scripps Benthic Invertebrate Collection, and Martin Tresguerres for the use of the Zeiss AxioObserver Z1 microscope.

LITERATURE CITED

Aiyar RG, Alikunhi KH. 1940. On a new pisionid from the sandy beach, Madras. Rec Ind Mus 42:89–107.

Arnold SJ. 1983. Morphology, performance and fitness. Amer Zool 23:347–361.

Ashworth JH. 1901. The anatomy of Scalibregma inflatum, Rathke. Q J Microsc Sci 2:237–309.

Ashworth JH. 1904. Memoir on Arenicola. The lugworm. Trans Liverpool Biol Soc 18:209–326.

Bellan G, Dauvin J-C. 1991. Phenetic and biogeographic relationships in Ophelia (Polychaeta, Opheliidae). Bull Mar Sci 48:544–558.

Blake JA. 2000. 7. Family Opheliidae Malmgren, 1867. In: Blake JA, Hilbig B, Scott PH, editors. Taxonomic Atlas of the Benthic Fauna of the Santa Maria Basin and Western Santa Barbara Channel, Vol. 7. The Annelida part 4 Polychaeta: Flabelligeridae to Sternaspidae. Santa Barbara: Santa Barbara Museum of Natural History. pp 145–168.

Bleidorn C. 2005. Phylogenetic relationships and evolution of Orbiniidae (Annelida, Polychaeta) based on molecular data. Zool J Linn Soc 144:59–73.

Bleidorn C, Vogt L, Bartolomaeus T. 2003. New insights into polychaete phylogeny (Annelida) inferred from 18S rDNA sequences. Mol Phylogenet Evol 29:279–288.

Brown RS. 1938. The anatomy of the polychaete Ophelia cluthensis McGuire 1935. P Roy Soc Edinb B 58:135–160.

Carr CM, Hardy SM, Brown TM, Macdonald TA, Hebert PDN. 2011. A trioceanic perspective: DNA barcoding reveals geographic structure and cryptic diversity in Canadian polychaetes. PLoS One 6:e22232.

Clark RB. 1964. Dynamics in Metazoan Evolution: The Origin of the Coelom and Segments. Oxford: Clarendon Press. p 313.

Clark RB, Clark ME. 1960. The ligamentary system and the segmental musculature of Nephtys. Q J Microsc Sci 3:149–176.

Clark RB, Cowey JB. 1958. Factors controlling the change of shape of certain nemertean and turbellarian worms. J Exp Biol 35:731–748.

Clark RB, Hermans CO. 1976. Kinetics of swimming in some smooth-bodied polychaetes. J Zool Lond 178:147–159.

Clifton HE, Thompson JK. 1978. Macaronichnus segregatis: A feeding structure of shallow marine polychaetes. J Sediment Petrol 48:1293–1302.

Colgan DJ, Mclauchalan A, Wilson GDF, Livingston SP, Edgecombe GD, Macaranas J, Cassis G, Gray MR. 1998. Histone H3 and U2 snRNA DNA sequences and arthropod molecular evolution. Aust J Zool 46:419–437.

Dales RP. 1962. The polychaete stomodeum and the interrelationships of the families of Polychaeta. P Zool Soc Lond 139:389–428.

Dauvin J-C, Bellan G. 1994. Systematics, ecology and biogeographical relationships in the subfamily Travisiinae (Polychaeta, Opheliidae). In: Dauvin JC, Laubier L, Reish DJ, editors. Actes de la 4éme Conférence Internationals des Polychétes, Vol. 162. Angers: Mém Mus Natl Hist Nat. pp 169–184.

Dorgan KM, Jumars PA, Johnson B, Boudreau BP, Landis E. 2005. Burrow extension by crack propagation. Nature 433: 475–475.

Dorgan KM, Jumars PA, Johnson B, Boudreau BP. 2006. Macrofaunal burrowing: The medium is the message. Oceanogr Mar Biol Ann Rev 44:85–121.

Dorgan KM, Law CJ, Rouse GW. 2013. Meandering worms: Mechanics of undulatory burrowing in muds. Proc R Soc B 280:20122948.

Eisig H. 1887. Monographie der Capitelliden des Gofes von Neapel und der angrenzenden meres-abschnitte nebst untersuchungen zur vergleichenden anatomie und physiologie. Fauna und Flora des Golfes von Neapel und der angrenzenden Meeresabschnitte, Vol. 16. Berlin: Friedländer. pp 1–906.

Elder HY. 1973. Direct peristaltic progression and the functional significance of the dermal connective tissues during burrowing in the polychaete Polyphysia crassa (Oersted). J Exp Biol 58:637–655.

Elder HY. 1980. Peristaltic mechanisms. In: Elder HY, Trueman ER, editors. Aspects of Animal Movement. Cambridge: University Press. pp 71–92.

Elder HY, Hunter RD. 1980. Burrowing of Priapulus caudatus (Vermes) and the significance of the direct peristaltic wave. J Zool 191:333–351.

Fauchald K, Jumars PA. 1979. The diet of worms: A study of polychaete feeding guilds. Oceanogr Mar Biol Ann Rev 17: 193–284.

Fauchald K, Rouse GW. 1997. Polychaete systematics: Past and present. Zool Scr 26:71–138.

Fraipont J. 1887. Le genre Polygordius. Fauna und Flora des Golfes von Neapel, Vol. 14. Berlin: Friedländer. pp 1–130.

Gardiner SL. 1992. Polychaeta: General organization. In: Harrison FW, Gardiner SL, editors. Microscopic Anatomy of Invertebrates. Vol. 7. Annelida. New York: Wiley-Liss. pp 19–52.

Giard MA. 1880. On the affinities of the genus *Polygordius* with the annelids of the family Opheliidae. Ann Mag Nat Hist, Ser 5, 6:324–326.

Giribet G, Carranza S, Baguna J, Riutort M, Ribera C. 1996. First molecular evidence for the existence of a Tardigrada plus Arthropoda clade. Mol Biol Evol 13:76–84.

Giribet G, Carranza S, Ruitort M, Baguna J, Ribera C, 1999. Internal phylogeny of the Chilopoda (Myriapoda, Arthropoda) using complete 18S rDNA and partial 28S rDNA sequences. Philos Trans R Soc B Biol Sci 354:215–222.

Gray J, Lissmann HW. 1938. Studies in Animal Locomotion VII. Locomotory reflexes in the earthworm. J Exp Biol 15: 506–517.

Hall KA, Hutchings PA, Colgan DJ. 2004. Further phylogenetic studies of the Polychaeta using 18S rDNA sequence data. J Mar Biol Assoc UK 84:949–960.

Harris JE, Crofton HD. 1957. Structure and function in the nematodes: Internal pressure and cuticular structure in Ascaris. J Exp Biol 34:116–130.

Harris T. 1994. The functional significance of blood plexuses in the ecology of *Ophelia bicornis* Savigny. In Dauvin JC, Laubier L, Reish, DC, editors. Actes de la 4éme Conférence internationals des Polychétes, Vol. 162. Angers: Mém Mus Natl Hist Nat. pp 57–63.

Hartman O. 1965. Deep-water benthic polychaetous annelids off New England to Bermuda and other North Atlantic areas. Allan Hancock Occas Pap 28:1–378.

Hartman O, Fauchald K. 1971. Deep-water benthic polychaetous annelids off New England to Bermuda and other North Atlantic Areas. Part II. Allan Hancock Monogr Mar Biol 6:1–327.

Hartmann-Schröder G. 1958. Zur morphologie der Opheliiden (Polychaeta sedentaria). Z Wiss Zool 161:84–143.

Hermans CO, 1978. Metamorphosis in the opheliid polychaete *Armandia brevis*. In: Chia FS, Rice ME, editors. Settlement and metamorphosis of marine invertebrate larvae. New York: Elsevier. pp 113–126.

Hunter RD, Moss VA, Elder HY. 1983. Image analysis of the burrowing mechanisms of Polyphysia crassa (Annelida: Polychaeta) and Priapulus caudatus (Priapulida). J Zool Lond 199:305–323.

Hutchings P, Murray A. 1984. Taxonomy of polychaetes from the Hawkesbury River and the Southern estuaries of New South Wales, Australia. Rec Austr Mus Sup 3:1–118.

Irschick DJ, Garland Jr, T. 2001. Integrating function and ecology in studies of adaptation: investigations of locomotor capacity as a model system. Annu Rev Ecol Syst 32:367–396.

Jördens J, Struck T, Purschke G. 2004. Phylogenetic inference regarding Parergodrilidae and Hrabeiella periglandulata ('Polychaeta', Annelida) based on 18S rDNA, 28S rDNA, and COI sequences. J Zool Syst Evol Research 42:270–280.

Katoh M, Kuma M. 2002. MAFFT: a novel method for rapid multiple sequence alignment based on fast Fourier transform. Nucleic Acids Res 30:3059–3066.

Kier WM. 2012. The diversity of hydrostatic skeletons. J Exp Biol 215:1247–1257.

Kier WM, Smith KK. 1985. Tongues, tentacles and trunks: the biomechanics of movement in muscular-hydrostats. Zool J Linn Soc-Lond 83:307–324.

Kohn AJ, Blahm AM. 2005. Anthropogenic effects on marine invertebrate diversity and abundance: Intertidal in fauna along an environmental gradient at Esperance, Western Australia. In: Wells FE, Walker DI, Kendrick GA, editors. The Marine Flora and Fauna of Esperance, Western Australia. Perth: Western Australia Museum. pp 1–23.

Lanzavecchia G, Eguileor M, Valvassori R. 1988. Muscles. In: Westheide W, Hermans CO, editors. The Ultrastructure of Polychaeta (Microfauna Marina), Vol. 4. Cleveland: Zubal Books. pp 71–88.

Lauder G. 1990. Functional morphology and systematics: studying functional patterns in an historical context. Annu Rev Ecol Systm 21:317–340.

Law CJ, Dorgan KM, Rouse GW. 2013. Validation of three sympatric Thoracophelia species (Annelida: Opheliidae) from Dillon Beach, California using mitochondrial and nuclear DNA sequence data. Zootaxa 3608:67–74.

Lehmacher C, Fiege D, Purschke G. 2013. Immunohistochemical and ultrastructural analysis of the muscular and nervous systems in the interstitial polychaete *Polygordius appendiculatus* (Annelida). Zoomorphology. doi:10.1007/s00435-013-0203-6

Maddison WP, Maddison DR. 2011. Mesquite: A modular system for evolutionary analysis. Version 2.75. Accessed on Feburary 21, 2011. Available at: http://mesquiteproject.org.

Martinez A, Di Domenici M, Worsaae K. 2013. Evolution of cave *Axiokebuita* and *Speleobregma* (Scalibregmatidae, Annelida). Zool Scripta. doi:10.1111/zsc.12024.

Matsui GY, Volkenborn N, Polerecky L, Henne U, Wethey DS, Lovell CR, Woodin SA. 2011. Mechanical imitation of bidirectional bioadvection in aquatic sediments. Limnol Oceanogr Methods 9:84–96.

McConnaughey DH, Fox DL. 1949. The anatomy and biology of the marine polychaete Thoracophelia mucronata (Treadwell) Opheliidae. Univ Calif Publ Zool 47:319–340.

McIntosh WC. 1875. On a new example of the Opheliidae *Linotrypane apogon* from Shetland. Proc R Soc Edinb B 8:386–390.

Moore JP. 1909. Polychaetous annelids from Monterey Bay and San Diego, California. Proc Acad Nat Sci Phila 61:235–295.

Murphy EAK, Dorgan KM. 2011. Burrow extension with a proboscis: mechanics of burrowing by the glycerid Hemipodus simplex. J Exp Biol 214:1017–1027.

Murray L, Tanzer M, Cookie P. 1981. Nereis cuticle collagen: Relationship of fiber ultrastructure to biochemical and biophysical properties. J Ultrastruct Res 76:27–45.

Nogueira JMM, Hutchings PA, Fukuda MV. 2010. Morphology of terebelliform polychaetes (Annelida: Polychaeta: Terebelliformia), with a focus on Terebellidae. Zootaxa 2460:1–185.

Norlinder E, Nygren A, Wiklund H, Pleijel F. 2012. Phylogeny of scale-worms (Aphroditiformia, Annelida), assessed from 18SrRNA, 28SrRNA, 16SrRNA, mitochondrial cytochrome c oxidase subunit I (COI), and morphology. Mol Phylogenet Evol 65:490–500.

Okuda S. 1936. Description of a new sedentary polychaete, *Thoracophelia ezoensis* n. sp. Proc Imper Acad 12:201–202.

Palumbi SR. 1996. Nucleic acids II: The polymerase chain reaction. In: Hillis DM, Moritz C, Mable BK, editors. Molecular Systematics, 2nd ed. Sunderland: Sinauer. pp 205–247.

Paul C, Halanych KM, Tiedemann R, Bleidorn C. 2010. Molecules reject an opheliid affinity for Travisia (Annelida). Syst Biodivers 8:507–512.

Persson J, Pleijel F. 2005. On the phylogenetic relationships of Axiokebuita, Travisia and Scalibregmatidae (Polychaeta). Zootaxa 998:1–14.

Purschke G, Ding Z, Müller MC. 1995. Ultrastructural differences as a taxonomic marker: The segmental ocelli of Polyophthalmus pictus and Polyophtahmlus qingdaoensis sp. n. (Polychaeta, Opheliidae). Zoomorphology 115:229–241.

Purschke G, Müller MCM. 2006. Evolution of body wall musculature. Integr Comp Biol 46:497–507.

Ramey PA, Fiege D, Leander BS. 2006. A new species of Polygordius (Polychaeta: Polygordiidae): From the inner continental shelf and in bays and harbours of the north-eastern United States. J Mar Biol Ass UK 86:1025–1034.

Roche C, Lyons DO, Farñas Franco J, O'Connor B. 2007. Benthic surveys of sandbanks in the Irish Sea. Irish Wildlife Manuals No. 29. Dublin: National Parks and Wildlife Service. p 48.

Rota E, Carchini G. 1999. A new Polygordius (Annelida: Polychaeta) from Terra Nova Bay, Ross Sea, Antarctica. Polar Biol 21:201–213.

Rouse GW, Pleijel F. 2001. Polychaetes. New York: Oxford University Press. p 354.

Rousset V, Pleijel F, Rouse GW, Erséus C, Siddall ME. 2007. A molecular phylogeny of annelids. Cladistics 23:41–63.

Rueckert S, Leander BS. 2009. Phylogenetic position and description of Rhytidocystis cyamus sp. n. (Apicomplexa, Rhytidocystidae): A novel intestinal parasite of the north-eastern Pacific 'stink worm' (Polychaeta, Opheliidae, Travisia pupa). Mar Biodiv 39:227–234.

Ruthensteiner B. 2008. Soft Part 3D visualization by serial sectioning and computer reconstruction. Zoosymposia 1:63–100.

Santos CSG, Nonato EF, Petersen ME. 2004. Two new species of Opheliidae (Annelida: Polychaeta): Euzonus papillatus sp. n. from a northeastern Brazilian sandy beach and Euzonus mammillatus sp. n. from the continental shelf of southeastern Brazil. Zootaxa 478:1–12.

Seymour MK. 1976. Pressure differences on adjacent segments and movement of septa in earthworm locomotion. J Exp Biol. 64:743–750.

Silva GS. 2007. Filogeniade Opheliidae (Annelida:Polychaeta), [dissertation]. Brazil: Universidade Federal do Paraná. p 95.

Spurr AR. 1969. A low-viscosity epoxy resin embedding medium for electron microscopy. J Ultrastruct Res 26:31–43.

Stamatkis A. 2006. RAxML-VI-HPC: Maximum likelihood-based phylogenetic analyses with thousands of taxa and mixed models. Bioinformatics 22:2688–2690.

Struck TH, Purschke G, Halanych KM. 2006. Phylogeny of Eunicida (Annelida) and exploring data congruence using a Partition Addition Bootstrap Alteration (PABA) Approach. Syst Biol 55:1–20.

Struck TH, Nesnidal MP, Purschke G, Halanych KM. 2008. Detecting possibly saturated positions in 18S and 28S sequences and their influence on phylogenetic reconstruction of Annelida (Lophotrochozoa). Mol Phylogenet Evol 48: 628–645.

Struck TH, Paul C, Hill N, Hartmann S, Hosel C, Kube M, Lieb B, Meyer A, Tiedemann R, Purschke G, Bieidorn C. 2011. Phylogenomic analyses unravel annelid evolution. Nature 471:95–98.

Swofford DL. 2002. PAUP*. Phylogenetic Analysis Using Parsimony (* and other methods). Version 4.0b10. Sunderland: Sinauer.

Trueman ER. 1966. The mechanism of burrowing in the polychaete worm, Arenicola marina. Biol Bull 131:369–377.

Trueman ER. 1978. Locomotion. In: Mill PJ, editors. The Physiology of Annelids. New York: Academic Press. pp 243–269.

Tzetlin AB. 1987. Structural peculiarities of Pisionidens tchesunovi (Polychaeta) and their possible significance. Zoologisceskij Zurnal 66:1454–1462.

Tzetlin AB, Filippova AV. 2005. Muscular system in polychaetes (Annelida). Hydrobiologia 535/536:113–126.

Tzetlin AB, Purschke G. 2005. Pharynx and intestine. Hydrobiologia 535/536:199–225.

Tzetlin AB, Zhadan A. 2009. Morphological variation of axial nonmuscular proboscis types in the Polychaeta. Zoosymposia 2:415–427.

Uebelacker, JM, Johnson, PG. 1984. Taxonomic guide to the polychaetes of the Northern Gulf of Mexico. Final Report to the Minerals Management Service, contract 14-12-001–29091. 7 Vols. Barry A. Vittor & Associates, Inc: Mobile, Alabama.

Wainwright PC, Mehta RS, Higham TE. 2008. Stereotypy, flexibility and coordination: Key concepts in behavioral functional morphology. J Exp Biol 211:3523–3528.

Wainwright SA, Briggs WD, Currey JD, Gosline JM. 1976. Mechanical design in organisms. Princeton: Princeton University Press, p 423.

Wells GP. 1954. The mechanism of proboscis movement in Arenicola. Q J Microsc Sci 3:251–270.

Wells GP. 1961. How lugworms move. In: Ramsey JD, Wigglesworth VB, editors. The Cell and the Organism. Cambridge: Cambridge University Press. pp 209–233.

Woodin SA. 1974. Polychaete abundance patterns in a marine soft-sediment environment: The importance of biological interactions. Ecol Monogr 44:171–187.

Worsfold T. 2006. Identification guides for the NMBAQC Scheme: 1. Scalibregmatidae (Polychaeta) from shallow seas around the British Isles. Porcupine Marine Natural History Society Newsletter 20:15–18.